Block toppling stability in the case of rock blocks with rounded edges

Manuscript Details

Manuscript number	ENGEO_2017_1239_R1
Title	Block toppling stability in the case of rock blocks with rounded edges
Article type	Research Paper

Abstract

A characteristic feature of spheroidal weathering is the rounding of rock block edges, which affects the mechanical stability of slender rock blocks and, consequently, that of slopes prone to toppling. We analysed the influence of this erosion phenomenon on block toppling stability, first discussing the geological environments that produce this kind of phenomena and then reviewing classic limit equilibrium equations for block toppling that account for the role played by rounded edges. On the basis of this approach, it is clear that rounded edges do not greatly affect stability against sliding. However, since the equation to compute stability against toppling tends to overestimate the stability of slopes with round-edged slender blocks, we propose a modification that results in a more accurate estimation. In physical model testing in the laboratory, we compared results for sharp-edge block models and artificially weathered rounded-edge blocks, confirming our formulated hypothesis and enabling us to explain the failure of sets of a small number of not-so-slender blocks. Fieldwork case studies confirm that rounded edges may play a role in stability against toppling. We suggest that our proposed approach may be an appropriate tool to take this effect into account.

Keywords	Block toppling; spheroidal weathering; rock slope stability; limit equilibrium; physical modelling.
Taxonomy	Applied Geomorphology, Rock Mechanics

Corresponding Author	Ignacio Pérez-Rey
Corresponding Author's Institution	University of Vigo
Order of Authors	Leandro R. Alejano, Carlota Sánchez-Alonso, Ignacio Pérez-Rey, Javier Arzua, Elena Alonso, Javier González, Luisa Beltramone, anna maria ferrero
Suggested reviewers	Juan Ramon Vidal Romani, Resat Ulusay, Richard E. Goodman, Jose Muralha

Block toppling stability in the case of rock blocks with rounded edges

Leandro R. Alejano, Carlota Sánchez-Alonso, Ignacio Pérez-Rey, Javier Arzúa, Elena Alonso, Javier González, Luisa Beltramone & Anna María Ferrero

HIGHLIGHTS

1. Spheroidal weathering and its potential influence on slope stability is studied
2. The effect of rounded edges on block stability against toppling is analysed
3. Some physical modelling has been developed to assess the role of this effect
4. Equations accounting for rounding corners to study toppling stability are proposed
5. Fieldwork case studies illustrates the relevance of the approach.

Block toppling stability in the case of rock blocks with rounded edges

Leandro R. Alejano[1], Carlota Sánchez–Alonso[1,4], Ignacio Pérez–Rey[1], Javier Arzúa[1], E. Alonso[1], Javier González[1,3], Luisa Beltramone[4] & Anna María Ferrero[4]

[1]*Department of Natural Resources and Environmental Engineering, University of Vigo, Vigo, Spain.*

[2]*Delft University of Technology (TU Delft), Delft, The Netherlands.*

[3]*Universidad Católica del Norte, Antofagasta, Chile.*

[4]*Department of Earth Science, University of Turin, Turin, Italy.*

Abstract

A characteristic feature of spheroidal weathering is the rounding of rock block edges, which affects the mechanical stability of slender rock blocks and, consequently, that of slopes prone to toppling. We analysed the influence of this erosion phenomenon on block toppling stability, first discussing the geological environments that produce this kind of phenomena and then reviewing classic limit equilibrium equations for block toppling that account for the role played by rounded edges. On the basis of this approach, it is clear that rounded edges do not greatly affect stability against sliding. However, since the equation to compute stability against toppling tends to overestimate the stability of slopes with round-edged slender blocks, we propose a modification that results in a more accurate estimation.

In physical model testing in the laboratory, we compared results for sharp-edge block models and artificially weathered rounded-edge blocks, confirming our formulated hypothesis and enabling us to explain the failure of sets of a small number of not-so-slender blocks. Fieldwork case studies confirm that rounded edges may play a role in stability against toppling. We suggest that our proposed approach may be an appropriate tool to take this effect into account.

Keywords: Block toppling, spheroidal weathering, rock slope stability, limit equilibrium, physical modelling.

Corresponding author: iperez@uvigo.es

1. Introduction

Toppling failure mechanisms tend to occur in slopes in rock masses containing a discontinuity set striking more or less parallel to the slope and dipping towards it. Although slope instability failures associated with toppling are not easy to identify, detailed analyses have shown that this mechanism lies behind a good number of problems identified in rock cuts (De Freitas and Waters, 1973; Sagaseta et al., 2001), open pit mine walls (Sjöberg, 1999; Martin, 1990) and natural slopes (Giraud et al., 1990; Cruden and Hu, 1994; Gischig et al., 2011). Sjöberg (1995) suggests that this type of failure mechanism seems to be much more common than initially thought. A better understanding of toppling phenomena and its

features would therefore be very useful in improving understanding, prediction and management of this type of instability.

Ashby (1971), in a seminal study, first documented the occurrence of toppling in rock, whereas Goodman and Bray (1976) made the first serious attempt to analyse this type of failure. More than a simple failure mechanism, in fact, toppling phenomena could be involved in a number of processes that negatively affect the stability of a slope. A simplified classification provided by Goodman and Bray (1976) referred to block toppling, flexural toppling and block-flexural toppling.

However, more complex phenomena that combine toppling with other basic failure modes (circular, planar or wedge failure) do occur and were described, among others, by Hoek and Bray (1974) and Wyllie and Mah (2004). These include failure mechanisms with toppling failure and circular failure in the upper and lower parts, respectively, like those described by Alejano et al. (2010) and Manera Bassa et al. (2014), or in the lower and upper parts, respectively, like those described by Mohtarami et al. (2014) and Stead et al. (2006). Other combinations of simpler mechanisms include sliding and toppling failure in the upper and lower parts, respectively (Cravero et al., 2003), or in the lower and upper parts, respectively (Gu and Guang, 2016; Coulthard et al., 2001). Even more complex failures involving toppling combined with two other mechanisms have been described in the literature (Böhme et al., 2013; León-Buendía et al., 2014).

Unlike other simpler failure mechanisms (e.g., planar or wedge failure), toppling tends to be controlled by a good number of discontinuities with variable geometry, features and behaviour. It is therefore not surprising that our ability to accurately estimate the stability of these slopes is much more limited than for simple mechanisms.

Within this framework, we observed that blocks with rounded corners were more prone to toppling than blocks with sharp corners and a study explaining, quantifying and demonstrating this phenomenon in relation to a single block was reported in due course (Alejano et al., 2015). Here we describe an extension of that study that focuses on how rounded corners in blocks affect the stability of slopes prone to block toppling. This study can be considered an extrapolation of the Goodman and Bray (1976) approach to analysing the role played by round-edged blocks in stability.

Below we describe how the basic equations of the Goodman and Bray (1976) approach were modified to account for rounded corners and then the modified equations are applied to a number of analyses. We tested the validity of our approach by means of physical models and used the results to eventually explain how and why block toppling occurred in a moderately weathered granite rock formation in a mountain area of NW Spain.

2. Fundamentals

2.1. Analysis of a single block

Alejano et al. (2015) studied the influence of rounded corners on stability for a single rock block, indicating that, in the analytical solution for the factor of safety (FoS) against toppling of a single block with sharp edges (Eq. 1), stability depends solely on the slenderness of the block for a given inclination of the base (α).

$$FoS = \frac{M_{stab.}}{M_{overt.}} = \frac{W\cos\alpha\,\Delta x/2}{W\sin\alpha\,y_n/2} = \tan^{-1}\alpha\frac{\Delta x}{y_n} \quad (1)$$

This means that there is a critical inclination at which FoS = 1. The angle of failure can be physically observed in laboratory tilt tests, consisting of observing block behaviour on a progressively tilted surface.

The stability of blocks with rounded corners was analysed in different ways in Alejano et al. (2015): for specimens built by collating different pieces of the same rock, for artificially eroded blocks for which the radii of curvature were appropriately estimated and, finally, using a numerical approach and UDEC (Itasca, 2010). The analytical approach considered the radii of curvature of block corners by displacing the rotation axis and then calculating the moments in the computation of the FoS, as shown in Eq. 2 and Figure 1:

$$FoS = \frac{M_{stab.}}{M_{overt.}} = \frac{W\cos\alpha\left(\frac{\Delta x}{2} - r\right)}{W\sin\alpha\frac{y_n}{2}} = \tan^{-1}\alpha\left(\frac{\Delta x - 2r}{y_n}\right) \quad (2)$$

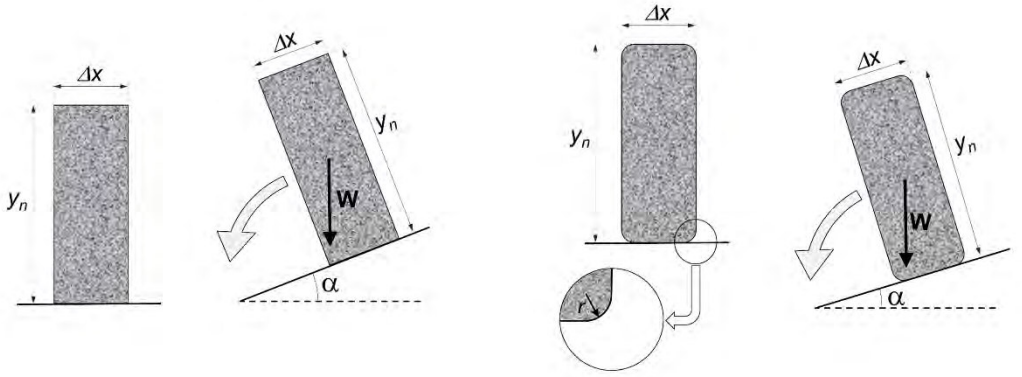

$$FoS = \frac{M_{stab}}{M_{overt}} = \frac{W\cos\alpha\frac{\Delta x}{2}}{W\sin\alpha\frac{Y_n}{2}} = \tan^{-1}\alpha\frac{\Delta x}{Y_n} \quad (1)$$

$$FoS = \frac{M_{stab}}{M_{overt}} = \frac{W\cos\alpha\left(\frac{\Delta x}{2} - r\right)}{W\sin\alpha\frac{Y_n}{2}} = \tan^{-1}\alpha\frac{\Delta x - 2r}{Y_n} \quad (2)$$

Figure 1. Factor of safety for a single block with sharp edges (1) and rounded edges (2).

2.2. Block toppling in rock slopes

In rock slopes, toppling involves the overturning of interacting columns or rock blocks around a fixed base (Goodman and Bray, 1976). This phenomenon usually happens when the strike of the rock mass joint sets (fault, stratification, etc) and of the slope are the same and when another set dips steeply into the rock mass. The most frequent failures of this kind are classified by Goodman and Bray (1976) as block toppling, flexural toppling and block flexural toppling. These mechanisms, illustrated in Figure 2, are briefly described below following Wyllie and Mah (2004).

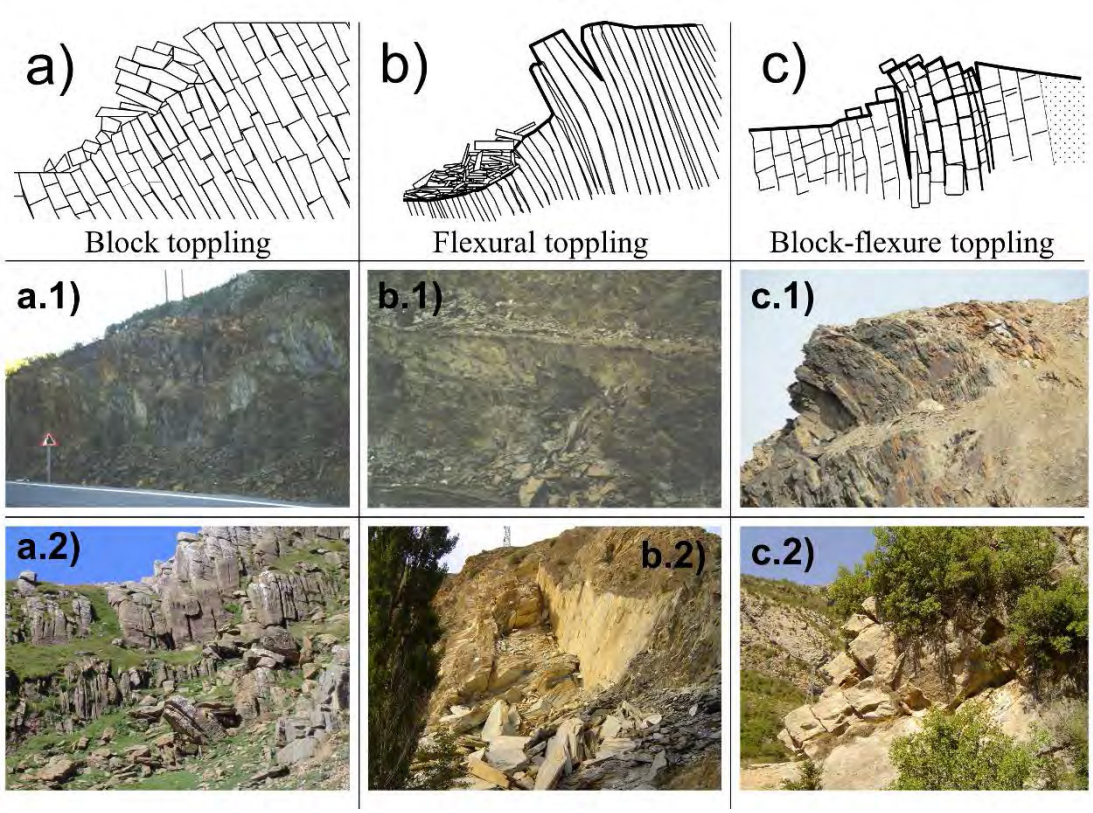

Figure 2. Common toppling failures as described by Willye and Mah (2004). a) Block toppling of slabs of rock with widely spaced normal joints: a.1) block toppling on a road in Salamanca (Spain); a.2) block toppling in the Pyrenees (Spain). b) Flexural toppling of slabs of rock dipping steeply into face: b.1) flexural toppling in a bench of the Tharsis copper open-pit mine in Huelva (Spain); b.2) flexural toppling near a riverbank in Sort near the Pyrenees (Spain). c) Block-flexural toppling characterized by pseudo-continuous flexure of long slabs through accumulated motions along various cross joints: c.1) block flexural toppling in a slate quarry in La Cabrera in León (Spain); c.2) block flexural toppling in a riverbank near Gerri de la Sal in Lleida (Spain).

Block toppling takes place in hard rock when individual blocks or columns are formed by two orthogonal joint sets, when the main set strikes parallel to the slope crest and dips steeply into the face. The upper blocks tend to topple and push forward on the short columns in the slope toe. Flexural toppling typically occurs in thinly bedded slate in which orthogonal jointing is not well developed; consequently, the basal plane is not as well defined as in block toppling. The general condition for flexural toppling is therefore when continuous columns of rock dipping steeply towards the slope break in flexure and tilt forward. Finally, block-flexural toppling is a complex mechanism characterized by pseudo-continuous flexure along long blocks that are divided by a number of cross-joints.

Cases of toppling have been widely reported in literature. Wyllie and Mah (2004) illustrated a case of pit-crest toppling that resulted in a circular failure in the upper slope. Hutchison et al. (2000), Coulthard et al. (2001) and Cravero et al. (2003) described complex failure mechanisms associated with toppling. Stead et al. (2006) reported and analysed a failure that occurred in the Delabole (UK) slate quarry that included toppling in the crest and circular failure in the lower part of the slope.

2.3. Geological framework

Weathering — the process by which rock deteriorates until eventually breaking down to a soil — is highly dependent on climatic influences (Selby, 1993). Weathering often works in from free surfaces where chemicals in water attack the parent rock, eventually leaving a framework or corestones of more or less fresh rock separated by weathered zones that are easily eroded (Ollier, 1975).

Joint sets found in rock masses are frequently orthogonal; two sets occur perpendicular to each other and at the same time perpendicular to some other planar fabric such as bedding, exfoliation or flow banding in an igneous pluton (Hencher, 2012b). When the spacing of one vertical joint set is smaller than that of the others, corestone development — due to weathering and subsequent denudation with finer weathered material — may produce rock block structures consisting of a series of contiguous sub-vertical round-edged blocks prone to toppling.

Although this kind of structure with toppling potential typically occurs in granite formations, it may also develop in other rock mass lithologies. Thus, similar rock structures may be produced by varying kinds of differential erosion and disintegration of sub-horizontally bedded and sub-vertically jointed sedimentary or volcanic rock in mountainous areas in temperate climate regions.

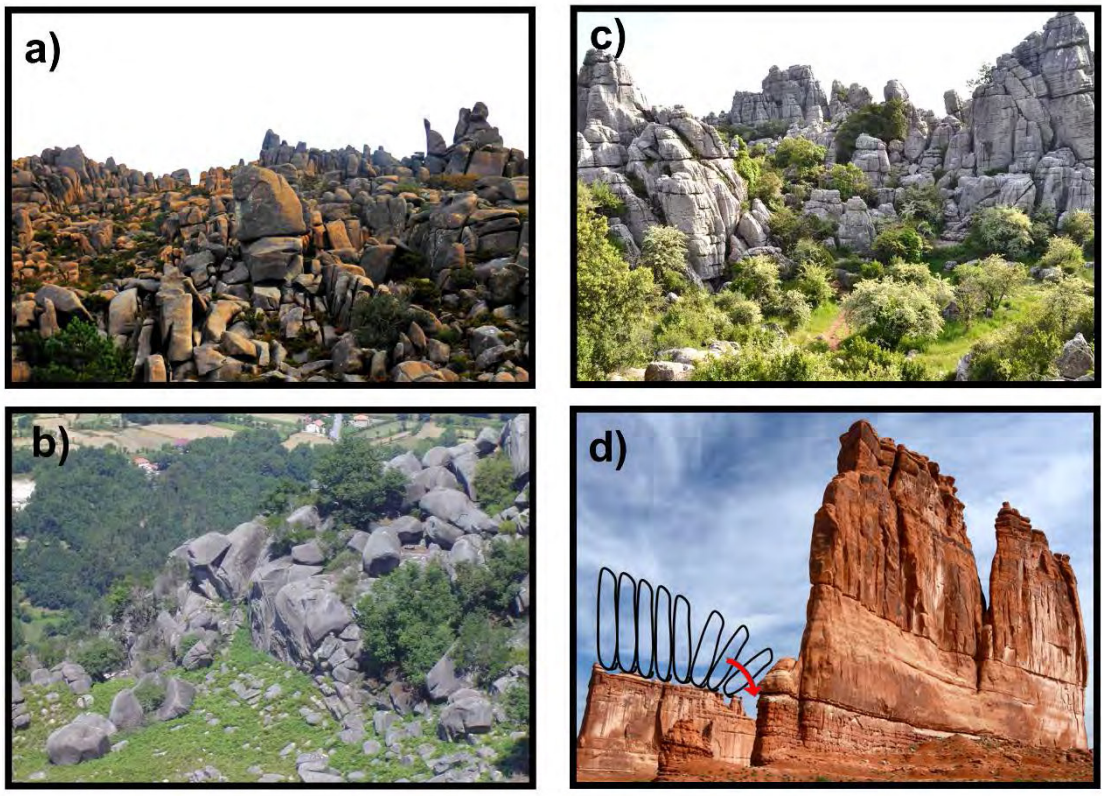

Figure 3. Examples of geological environments where the toppling phenomena under scrutiny may take place. a) Monte Pindo (A Coruña, Spain), b) Peneda Gêres National Park (Portugal), c) El Torcal de Antequera (Málaga, Spain), and d) Arches National Park (Utah, USA).

Some examples of toppled blocks in granite formations include Monte Pindo (Vidal Romaní, 1989) in the province of A Coruña in Spain and the Peneda Gerês National Park in Portugal (Vidal Romaní, 1990) (Figures 3.a and 3.b). Examples for other lithologies are El Torcal de Antequera karstic limestone formation in Málaga, Spain (Sanz de Galdeano, 1990) and the sandstone fins in Arches National Park in Utah, USA (Figures 3.c and 3.d). In these last formations, the rock pinnacles or fins were moulded by differential weathering and erosion of vertically jointed rock masses presenting horizontal beds of low-strength interbedded rock.

3. Analytical approach

3.1. Rounded corners in block toppling

Since rounded edges in blocks may appear in rock blocks in slopes prone to toppling, we propose an analytical approach to calculating the corresponding FoS based on first revisiting the limit equilibrium equations described in Goodman and Bray (1976). The analysis of a single block demonstrated that the impact of rounded corners on sliding mechanisms is negligible (Alejano et al, 2015). However, as illustrated in Figure 4, the rotation axis is displaced in toppling blocks.

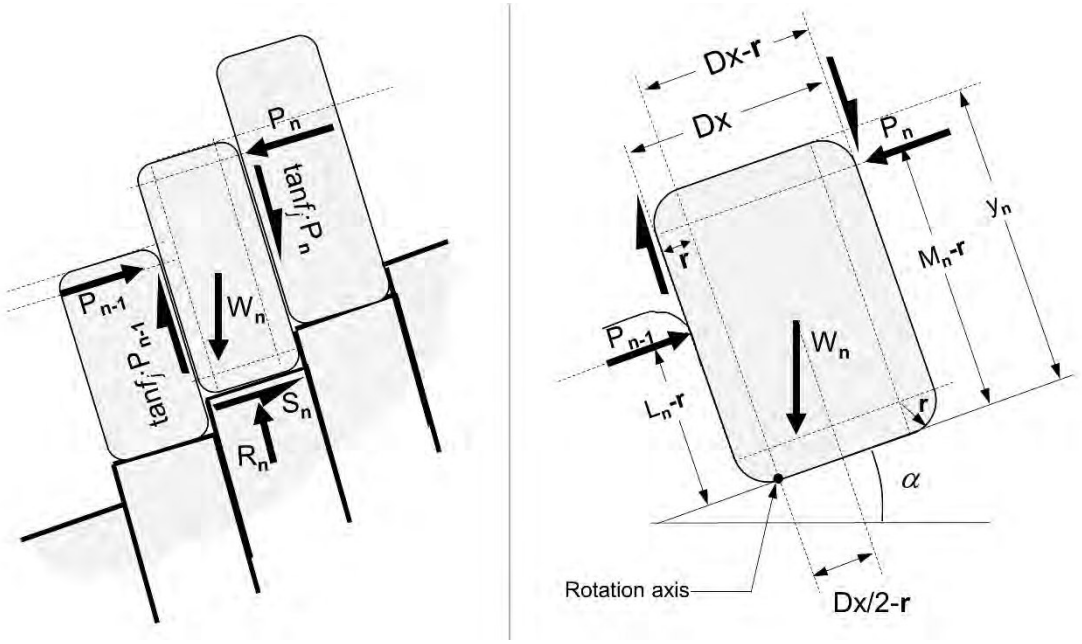

Figure 4. Geometry and forces acting on a block with rounded edges.

Proposed here is a modification of the equation used to calculate the force necessary to prevent a block from toppling, in which the moments are calculated taking into account the rounding of block edges. To simplify calculations, circular curvature of the edges is suggested as a hypothesis. The modified equation (Eq. 3) — used in further calculations for blocks with rounded edges — is as follows:

$$P_{n-1,t} = \frac{P_n \left[(M_n - r) - \tan\phi_j \cdot (\Delta x - r)\right] + \frac{W_n}{2} \left(y_n \cdot \sin\alpha - (\Delta x - 2r) \cdot \cos\alpha\right)}{L_n + r(\tan\phi_j - 1)} \quad (3)$$

3.2. Analysis of standard cases

With the modification represented by Eq. (3) in mind, repercussions for the stability of slopes were analysed. Variations in the FoS against the radii of curvature of the edges were evaluated for two standard cases from the literature, namely, Goodman and Bray (1976) and Alejano and Alonso (2005).

The Goodman and Bray (1976) example refers to a 92.5-m high slope composed of 16 x 10-m wide blocks. The specific weight of the rock was assumed as 25 kN/m^3. For a friction angle ϕ = 38.18° (for base and block contacts) the FoS of the slope was 1. The Alejano and Alonso (2005) example refers to a 10.95-m high slope composed of 12 x 1.75-m wide blocks, with the same specific weight as in the Goodman and Bray (1976) example. Two different friction angles were assumed for the calculations, one for the block bases and the other for the joints between blocks (ϕ_b=30^0 and ϕ_j=44^0, respectively). For these parameters the slopes were in limit equilibrium. Other geometrical parameters for both examples were as indicated in Figure 5.

With these two examples, starting from limit equilibrium with sharp edges, the FoS of the slopes were calculated for different radii of curvature of the corners. The results were then plotted in a graph for comparative purposes. In this graph — shown in Figure 6 — the radius of curvature was reflected as the ratio between the radius of curvature and block width ($r_c/\Delta x$). Computations were carried out up to the point when r_c was 30% of block width — a reasonable value given observations in the field. It can be readily observed that, from limit equilibrium, the FoS decreased to below 0.85 when corners became rounded. This would indicate that the rounding of rock block edges does indeed affect the stability of slopes with a relatively small number of blocks prone to toppling.

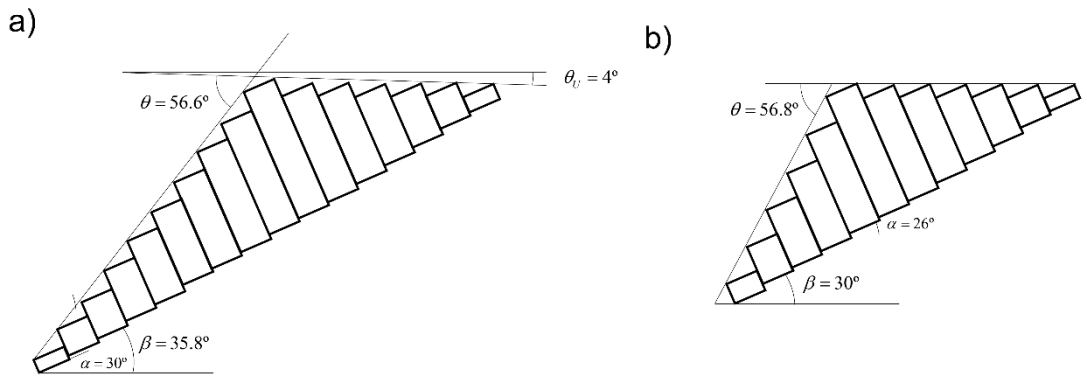

Figure 5. Geometrical parameters for the Goodman and Bray (1976) slope (a) and the Alejano and Alonso (2005) slope (b).

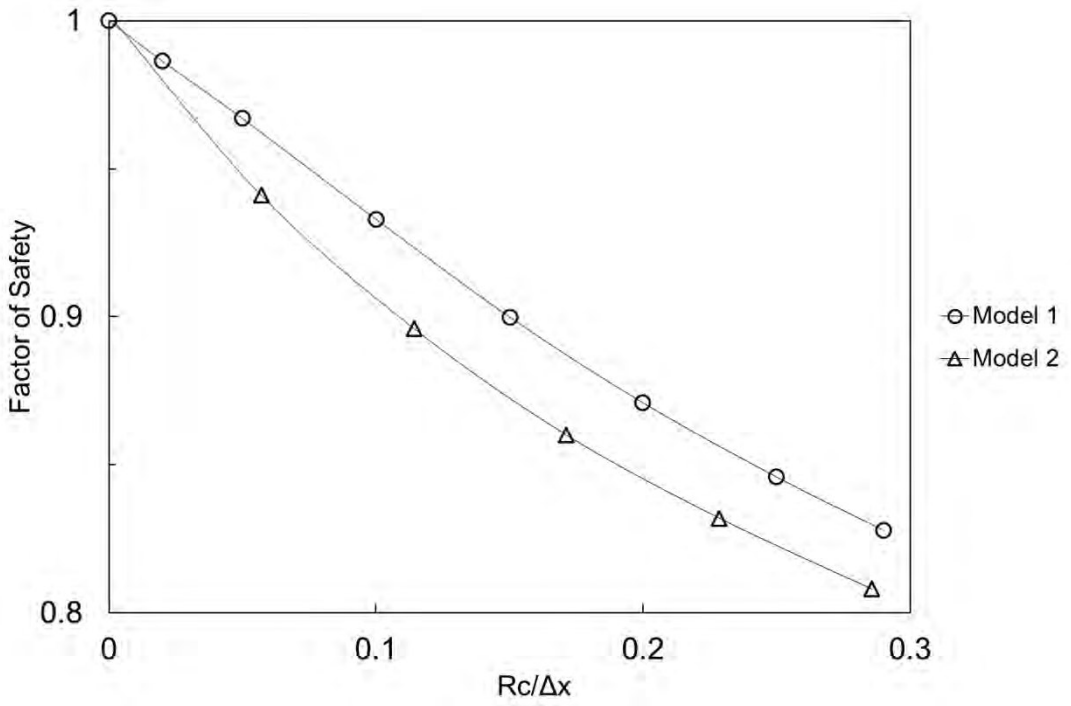

Figure 6. Variations in the factor of safety according to the radius of curvature to block width ratio, $r_c/\Delta x$.

4. Physical models

4.1. Introduction and description of the models

Experience acquired in wall slope failure cases — studied through physical modelling of stability for small-scale slopes formed of rock blocks with stability controlled by contact friction (Alejano et al., 2011) — suggested that a similar physical modelling approach could shed light on the phenomenon under scrutiny.

Taking the modified Eq. (3) into consideration, the block toppling mechanism was reproduced in the laboratory using two 10-block saw-cut Rosa Porriño granite models as illustrated in Figure 8. The models were cut from a 31-mm wide granite specimen, roughly finished on one side and polished on the other side. Two sets of 48.5-mm wide blocks were cut to heights of 15, 30, 45, 60, 75, 90, 105, 90, 75 and 60 mm. One set was left with saw-cut sharp edges and the other underwent 12 hours of mechanical weathering in a slake durability machine to obtain rounded edges.

Both models were tested on a tilt table (Alejano et al., 2012) using four different bases: a flat wooden base, a flat polished granite, a flat rough granite and, finally, a stepped wooden base consisting of 10 x 10.3-mm high and 31.19-mm wide steps (Figure 8). The tilt machine consists of a flat tilting surface controlled by an electric motor. A variable-frequency drive allows the tilting rate to be regulated and movement is controlled by means of three buttons (raise, tilt and stop).

Figure 7. Two sets of 10 blocks, with sharp edges (a) and with rounded edges (b).

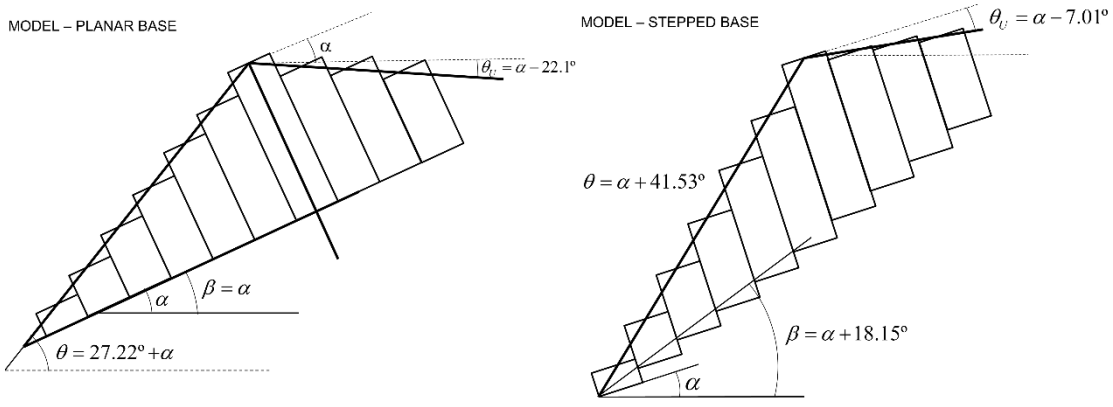

Figure 8. Geometrical parameters for the flat and stepped bases.

Reproducing the Goodman and Bray (1976) physical model meant that the inclination of the tilt table at limit equilibrium — i.e., the failure angle, α — could be predicted. Eq. (3) was used to assess the stability of the model of blocks with rounded corners.

4.2. Defining parameter measurements

The blocks were measured to obtain the parameters for the limit equilibrium calculations. These parameters were width, length, height, weight and submerged weight (to calculate density). Tables 1 and 2 list these measurements for sharp-edge and rounded-edge blocks, respectively.

For the rounded blocks, the radii of curvature were calculated following Alejano et al. (2015). Table 3 shows the geometrical and weight values of slab-like blocks (B-width, L-length and H-height) after slaking them for some hours to obtain rounded block edges. The operative radius of curvature is the radius at the mid-location of the edges. The value used to calculate limit equilibrium was the average of all the operative radii of curvature.

$$r_M = \frac{2}{3} r_c^{av} \tag{4}$$

Table 1. Geometrical and weight data for the sharp-edge blocks.

Block #	B	L	H	Weight	Submerged weight	Density from sunken weight
	[mm]	[mm]	[mm]	[g]	[g]	[g/cm^3]
1	31.21	47.74	15.66	60.13	37.36	2.64
2	31.06	47.77	30.36	116.64	72.2	2.62
3	31.10	47.56	47.50	169.73	104.85	2.62
4	31.17	47.89	59.34	229.4	141.86	2.62
5	31.23	47.64	75.36	290.37	179.61	2.62
6	31.37	47.92	89.84	349.8	216.4	2.62
7	31.35	47.90	104.31	404.7	250.18	2.62
8	31.33	48.14	89.50	349.04	215.76	2.62
9	31.20	47.65	74.42	285.97	178.83	2.67
10	31.13	47.65	59.97	230.16	142.44	2.62
					Average	2.63

Table 2. Geometrical and weight data for rounded-edge blocks.

Block #	B	L	H	Weight	Submerged weight	Density from sunken weight
	[mm]	[mm]	[mm]	[g]	[g]	[g/cm^3]
1	31.27	47.80	15.74	58.3	36.52	2.67
2	31.09	47.78	30.41	112.8	70.08	2.64
3	31.10	47.55	44.63	164.1	100.71	2.59
4	31.17	48.32	59.42	225.2	137.85	2.58
5	31.35	47.77	64.83	288.2	175.97	2.57
6	31.34	48.26	89.72	345.3	212.93	2.61
7	31.40	47.50	104.27	404.6	247.56	2.58
8	31.38	47.97	89.48	345.3	210.64	2.56
9	31.22	47.52	74.50	284.0	174.4	2.59
10	31.20	47.71	60.06	229.8	142.16	2.62
					Average	2.60

Table 3. Original and final weights of blocks after slaking and radius of curvature calculation results.

Block #	Weight of sharp-edge block	Weight of rounded-edge block	Weight loss	Average radius of circular rounding	Operative radius of curvature
	[g]	[g]	[%]	[mm]	[mm]
1	60.13	58.33	2.99	2.916	1.944
2	116.63	112.76	3.32	3.955	2.637
3	169.71	164.11	3.30	4.490	2.990
4	229.38	225.24	1.80	3.653	2.435
5	290.35	288.16	0.75	2.423	1.62
6	349.79	345.34	1.27	3.425	2.28
7	410.81	404.62	1.51	3.841	2.56
8	349.01	345.27	1.07	3.140	2.09
9	285.97	284.01	0.68	2.389	1.593
10	230.14	229.78	0.16	1.080	0.72
		Average	1.70	3.13	2.09
		Std. Dev.	1.14	0.983	

The main parameters affecting the results were the friction angles, which were estimated by means of tilt testing following the procedure described in Alejano et al. (2012). The friction angles were obtained for the contacts between the blocks and the different bases (ϕ_b) and for the joints (ϕ_j). Results between tests varied considerably, and there was also a decrease in friction angle results due to wear of the tilt surface (Hencher, 2012). Hence, the results of these tests should be considered as estimative. The tests were performed four times for each contact and physical model. The median was chosen as the estimated value given that outliers may well feature in this kind of test (Alejano et al., 2012).

Table 4. Friction angle estimates for contacts with different bases and for joints.

Test #	Sharp Edges				Rounded Edges			
	Wooden Base	Rough Granite	Polished Granite	Block Joints	Wooden base	Rough Granite	Polished Granite	Block Joints
1	26.8	23.9	18.5	18.2	26.8	20.3	23.5	24.9
2	32.3	22.1	22.0	17.8	26.7	18.5	19.3	27.5
3	26.4	20.9	16.0	19.9	23.6	21.6	19.7	27
4	25.9	17.9	17.6	21.6	25.1	21.2	17.5	26.2
Median	26.6	21.5	18.05	19.05	25.9	20.75	19.5	26.6
Average	27.85	21.2	18.52	19.37	25.55	20.4	20	26.4
St. Dev.	2.99	2.52	2.54	1.74	1.52	1.38	2.52	1.13

From the measurement data it was possible to calculate the failure angle and predict the inclination of the tilt table, α, at failure in order to compare theoretical and laboratory results. The geometrical parameters used in the calculations are shown in Figure 8 (above).

Note that all the angles depend on the inclination of the base (α). Predictions were computed using an Excel application (created by Carranza-Torres) that calculated slope FoS against toppling taking into account the rounding of rock block edges.

4.3. Tilt testing and results

For the tilt tests, the models were placed on the tilt table in contact, in turn, with the four different bases. Before placement, blocks were lightly wiped with a dry cloth and then they were slightly pushed against each other to force contact between blocks. Special attention was paid to positioning on the stepped wooden base to avoid block overhang.

The tilt table was raised at a rate of 10^0/min and stopped once block movement was observed. The inclination angle of the table at the moment of instability was recorded using a Leica Disto D5 laser electronic distance meter with precision to one decimal place. Each model was tested five times for each base. To compensate for possible deviations in cuts, the blocks were turned upside down and the procedure was repeated.

Tables 5-7 show the angles at which model failure occurred and, for comparative purposes, the theoretical predictions. Tables 5 and 6 show the results obtained for each model and test and Table 7 summarizes results according to the median for each set and also compares the laboratory failure angle results with theoretical FoS failure angle predictions according to the updated Goodman and Bray (1976) approach.

Table 5. Sharp-edge model results for four different bases.

Base	Flat Wooden		Rough Granite		Polished Granite		Stepped Wooden	
Position	Normal	Upside Down	Normal	Upside Down	Normal	Upside Down	Normal	Upside Down
1	21.8	21.9	20.4	21.1	18.2	17.9	19.2	18.9
2	21.4	20	21.6	21.3	18	18.5	18.7	18.8
3	21.3	20.5	20.1	19.9	14.6	15.4	19.2	18.5
4	21.9	22.1	20.4	20.2	17.5	17.1	18.7	18.5
5	21	20.2	19.9	20.4	15.1	17.5	18.8	18.8
Median	21.4	20.5	20.4	20.4	17.5	17.5	18.8	18.8
Average	21.48	20.94	20.48	20.58	16.68	17.28	18.92	18.7
St Dev	0.370	0.986	0.661	0.597	1.699	1.171	0.259	0.187

Table 6. Rounded-edge model results for four different bases.

Base	Flat Wooden		Rough Granite		Polished Granite		Stepped Wooden	
Position	Normal	Upside Down	Normal	Upside Down	Normal	Upside Down	Normal	Upside Down
1	19.40	17.10	17.80	18.30	15.50	16.60	16.40	15.80
2	19.70	19.30	14.70	16.70	13.40	17.40	20.00	15.20
3	19.60	17.10	18.60	17.40	14.40	17.40	16.30	16.50
4	20.00	17.00	17.50	18.20	15.10	17.40	16.60	15.60
5	18.60	20.00	17.90	18.70	12.20	18.30	16.60	16.10
Median	19.6	17.1	17.8	18.2	14.4	17.4	16.6	15.8
Average	19.46	18.1	17.3	17.86	14.12	17.42	17.18	15.84
St Dev	0.527	1.437	1.508	0.802	1.337	0.602	1.582	0.493

Table 7. Average values of results shown in Tables 5 and 6.

Base	Sharp-Edge Model			Rounded-Edge Model		
	Prediction	Results		Prediction	Results	
Flat Wooden	20.9	21.4	20.5	19.4	19.6	17.1
Rough Granite	19.4	20.4	20.4	17.9	17.8	18.2
Polished Granite	17.5	17.5	17.5	17.4	14.4	17.4
Stepped Wooden	18.7	18.8	18.8	16.6	16.6	15.8

4.4. Results interpretation in terms of FoS against toppling

To ensure a fair comparison between the physical model results and the theoretical predictions in terms of limit equilibrium, FoS values at failure were computed to evaluate the accuracy and precision of the results regarding the stability of the models.

Figures 9-12 graphically compare the predicted behaviour and laboratory results obtained for the sharp-edge models (SE, continuous lines) and rounded-edge models (RE, broken lines) for each of the four bases, depicting the predicted variation in the FoS against the inclination of the base (α). Individual observations are indicated by black circles and triangles and the mean of the two medians obtained for each set is indicated by a white circle or triangle. The FoS values were computed in an Excel spreadsheet application (created by Carranza-Torres) that calculated slope FoS against toppling taking into account the rounding of rock block edges.

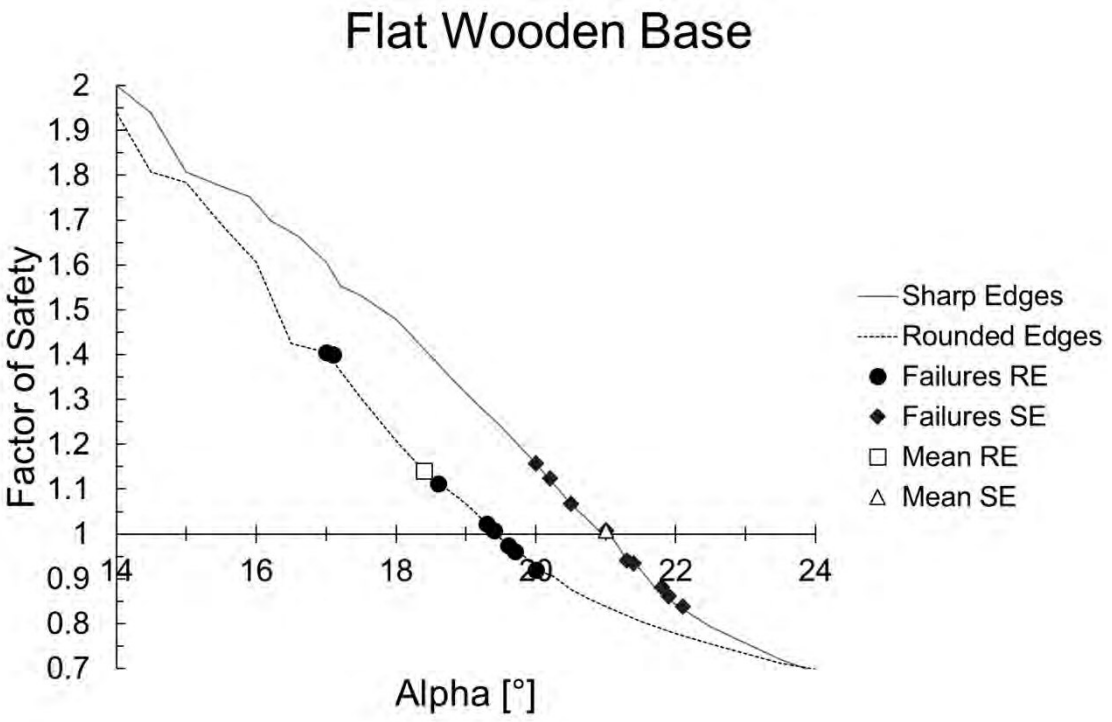

Figure 9. Model behaviour for the flat wooden base.

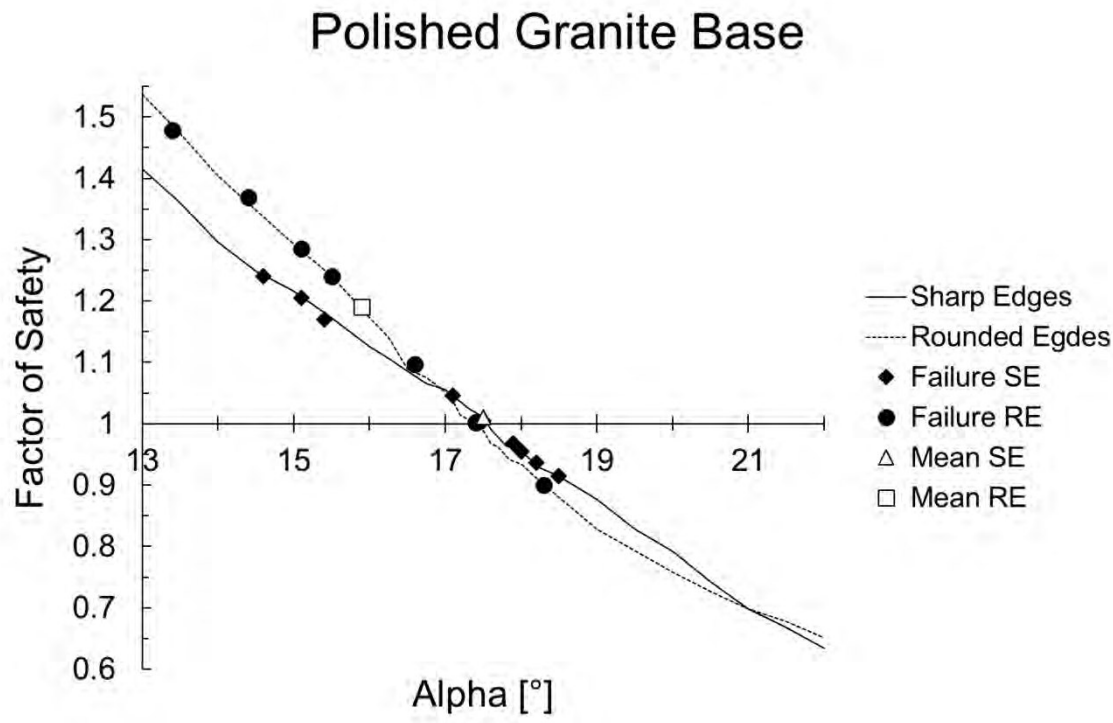

Figure 10. Model behaviour for the polished granite base.

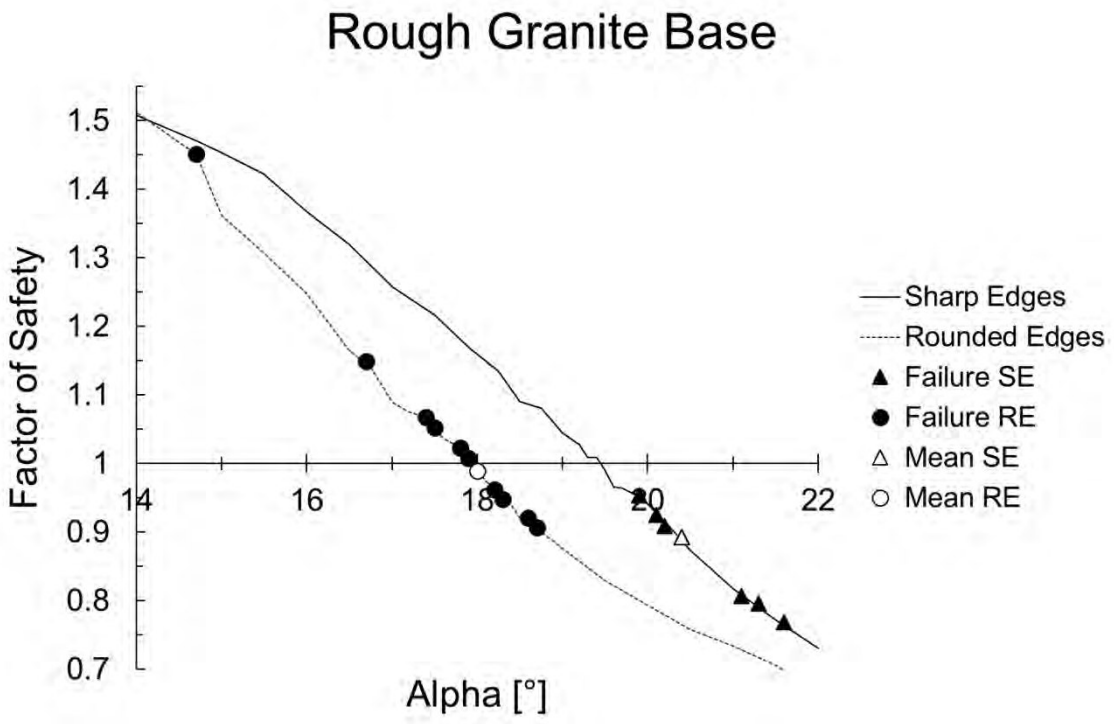

Figure 11. Model behaviour for the rough granite base.

It can be observed that results varied widely depending on the model and the base. The greatest variability occurred in the tests carried out on the polished base (standard deviation of around 1.5^0), indicating that in occasion, the model failed when the overall computed FoS was right off 1.5.

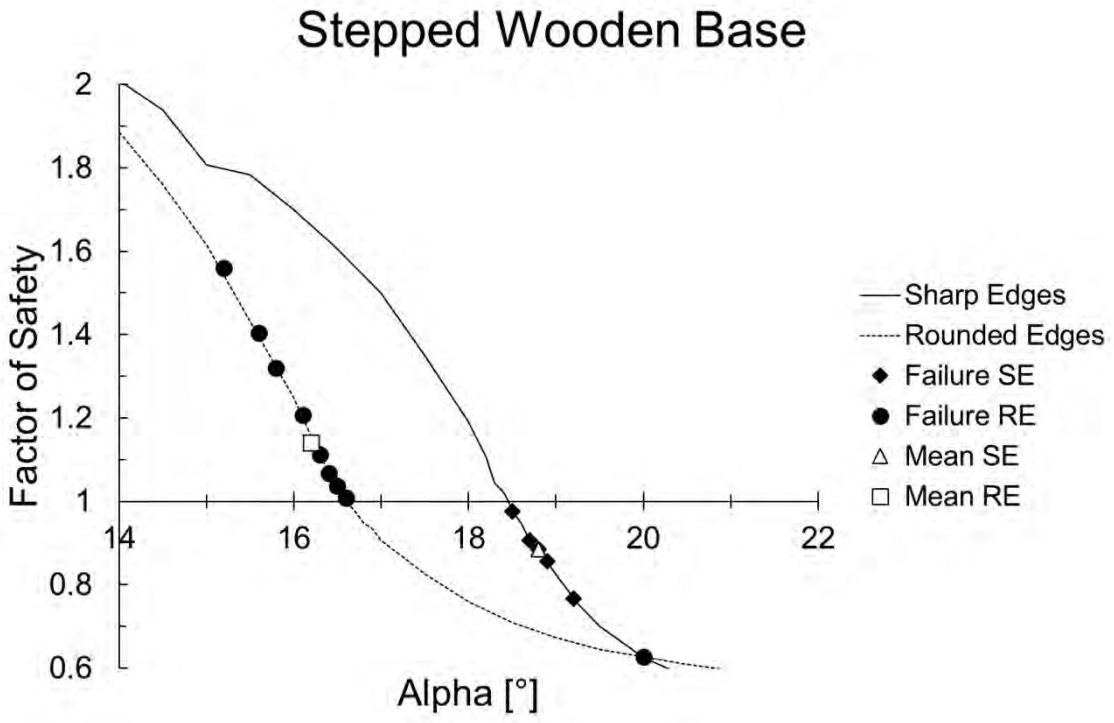

Figure 12. Model behaviour for the stepped wooden base.

The most consistent results were found for the rough granite base, with a standard deviation of 0.6^0 for sharp edges and 0.16^0 for rounded edges. However, in terms of measurement precision, it can be observed that the stability prediction regarding the sharp-edge model tends to be slightly underestimated, whereas that of the rounded-edge model tends to be overestimated. However, this level of variability is very small in comparison to that typically encountered in most rock engineering studies.

The fact that the mean values for the sharp-edge model were closer to the predicted values than the mean values for the rounded-edge model may be attributable to measurement error and forward estimates of actual operating radii of curvature.

4.5. Analysis and discussion of the failure mechanisms

When the failure mechanism of each block was analysed, the theoretical and laboratory approaches agreed almost completely for both the sharp-edge and rounded-edge models. Figure 13 depicts the models at the moment of failure and Table 8 compares the theoretically predicted failure mechanisms with the observed failure mechanisms.

It can be observed that the theoretical and laboratory approaches agreed, except in regard to the wooden bases for the rounded-edge models. For the stepped wooden base, Block 9 was predicted to topple yet remained stable in the laboratory model, and for the flat wooden base, block 3 was predicted to topple but instead slid. It can therefore be concluded that the predictions were quite reliable, indicating that the mechanism was well captured by the approach, even if some local variation in geometry or frictional response may have produced slight inaccuracies in numerical outputs (discussed further in the next section).

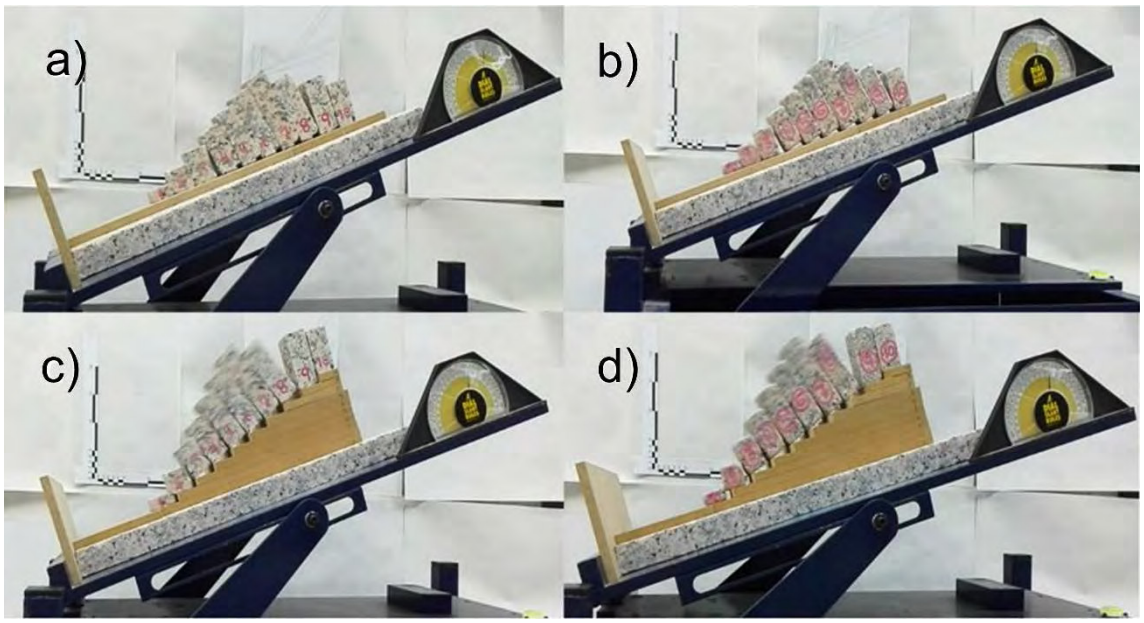

Figure 13. Four models at failure: a) sharp-edge model on flat wooden base, b) rounded-edge model on flat wooden base, c) sharp-edge model on stepped wooden base, and d) rounded-edge model on stepped wooden base.

Table 8. Summarized failure mechanisms for the models reflected in Figure 13. T stands for theoretical and L for laboratory.

Block	Sharp-Edge Models				Rounded-Edge Models			
	Flat Wooden Base		Stepped Wooden Base		Flat Wooden Base		Stepped Wooden Base	
	T	**L**	**T**	**L**	**T**	**L**	**T**	**L**
10	Stable	Stable	Stable	Stable	Stable	Stable	Stable	Stable
9	Toppling	Toppling	Stable	Stable	Toppling	Toppling	Toppling	Stable
8	Toppling	Toppling	Toppling	Toppling	Toppling	Toppling	Toppling	Toppling
7	Toppling	Toppling	Toppling	Toppling	Toppling	Toppling	Toppling	Toppling
6	Toppling	Toppling	Toppling	Toppling	Toppling	Toppling	Toppling	Toppling
5	Toppling	Toppling	Toppling	Toppling	Toppling	Toppling	Toppling	Toppling
4	Toppling	Toppling	Toppling	Toppling	Toppling	Toppling	Toppling	Toppling
3	Sliding	Sliding	Toppling	Toppling	Toppling	Sliding	Toppling	Toppling
2	Sliding	Sliding	Sliding	Sliding	Sliding	Sliding	Sliding	Sliding
1	Sliding	Sliding	Sliding	Sliding	Sliding	Sliding	Sliding	Sliding

4.6. Discussion of the laboratory results

The tests and calculations confirm that, as predicted, stability is reduced by the rounding of block edges. Our results indicate that rounded-edge models fail 2-3^0 before sharp-edge models.

It should be noted that where the geometry of the blocks is controlled and well known, as was the case here, the friction angle is the parameter that most influences the theoretical estimates. Therefore, prediction accuracy greatly relies on accurate calculations of the friction angle. However, friction angle precision in measurements was lower than that of the failure angle of the models. Since the standard deviation of the model outputs was smaller than that of the friction angle measurements, it can be concluded that the overall geometry compensated for the individual variations.

Failure for the polished granite base occurred when only block 1 or blocks 1 and 2 and not the whole model slid. This implies that even though the results were influenced by the overall geometry of the model more than by the friction angle, variations in the contacts may have significantly influenced overall model stability, especially when the predominant failure mechanism was sliding rather than toppling and the friction angle of the base was rather low. This means that the prediction and the results were in conflict. However, discarding those results meant that the prediction satisfactorily estimated the behaviour of the physical model.

As for prediction accuracy, this can be considered rather satisfactory, except for the rough granite base, where the discrepancy between predictions and results may be due to an underestimation of the friction angle of the base. Indeed, base friction angle measurements for this kind of surface are often erratic. For the rounded-edge model, even though predictions may differ slightly from the experimental results, they were still quite close to the observed values.

The values obtained for the polished granite base were much lower than the predicted values when the first couple of blocks slid first. The low friction angle in these contacts may

be due to the lower normal stress associated with the smaller size of these blocks. However, when the whole model failed, the failure angle was closer to the predicted value.

Finally, a possible source of error — other than that related to friction angle measurement — may have been a slight rounding of the blocks with sharp edges. Moreover, in line with observations by Alejano et al. (2015), for the stepped wooden base, block overhang may have influenced results and produced a lower failure angle. Additionally, possible imprecisions in measurements of the radii of curvature need to be acknowledged, along with irregularities in the circularity of the curved surfaces.

Summing up, it is evident that rounded block edges affect the overall stability of physical models, with laboratory failure angles for rounded-edge models dropping by $2\text{-}3^0$ compared to values for the sharp-edge blocks. It can therefore be reasonably concluded that artificial weathering of the rock blocks indeed influenced the stability of the rounded-edge model.

The proposed modified equation (Eq. 3) has been demonstrated to be quite accurate despite the variations in the friction angles attributable to external factors. Note also that precision was similar for both model types, with errors observed in the order of a mere 0.1^0 — a level of inaccuracy well below that typically found in rock mechanics practice and usually overcome when the FoS is applied to slope design.

5. Field evidence

Probably the most important implications of the studied mechanism refer to geological risk assessment for natural mountain slopes and geomorphology issues. Below we illustrate the role played by this erosion-triggered instability phenomenon, calculating the influence of weathering on block stability by studying blocks subject to toppling mechanisms where rounded edges played a relevant role.

To study the influence of block-edge rounding at field scale in natural slopes, we analysed different sets of blocks from Monte Pindo (also known as O Pindo), located in the municipality of Carnota, A Coruña, between the Rías Baixas and Cape Fisterra (NW Spain). Monte Pindo is part of one of the most representative granitic massifs of the late Variscan (Hercynian) orogeny. The rocks in this area are predominantly biotite granite, pink in colour with a medium to fine grit and largely isotropic.

The main characteristic of these granites is the presence of abundant discontinuities, generated during the last stages of the intrusion event when these rocks were not exposed to the surface (Pueyo–Morer et al., 1995). The massif is crossed by NE-SW and NNW-SSE vertical faults, several kms long, caused by a distension movement resulting from post-kinematic strains that created a dense set of blocks. Another set of discontinuities is represented by sheet joints, associated with the batholite structure in the area of the core of Mount Pindo (A Moa) — caused by its dome form (Twidale and Vidal–Romaní, 2005) and also a consequence of the elastic domain at this stage.

Chemical alteration moulded the lithology, with spheroidal weathering playing a primary role. Spheroidal weathering is also the form of weathering that most influenced this study. Jones (1859) described this type of weathering as percolating water flowing through fractures or cracks and decomposing adjacent rock masses. Since corners are attacked from

three sides, they are the most affected and become more spheroidal. Several theories describe the process such rocks undergo until eventually achieving their present shape.

The Monte Pindo area has a large number of weathered boulders, including toppled specimens, mostly single blocks (e.g., Figure 14), but also sets of blocks that had apparently experienced toppling failure (e.g., Figure 15).

Figure 14. Toppled single block on Monte Pindo (A Coruña, NW Spain).

Figure 15. Apparently toppled series of blocks showing rounded corners on Monte Pindo (A Coruña, NW Spain).

Although several series of toppled blocks were identified in situ, the geometry of some of them was too complex (influenced by three-dimensionality) to make straightforward stability calculations for demonstrative purposes. Two cases with a relatively simple geometry were selected for analysis, as described below.

5.1. Case study 1

The first case study referred to a set of four blocks (Figure 16). As found, two blocks were already toppled, but another rock was preventing them from falling to the ground, and yet another block lay on the ground. The possibility of a fifth block that had already fallen down the hill was also taken into account in calculations, although the likelihood of just four blocks produced more coherent results.

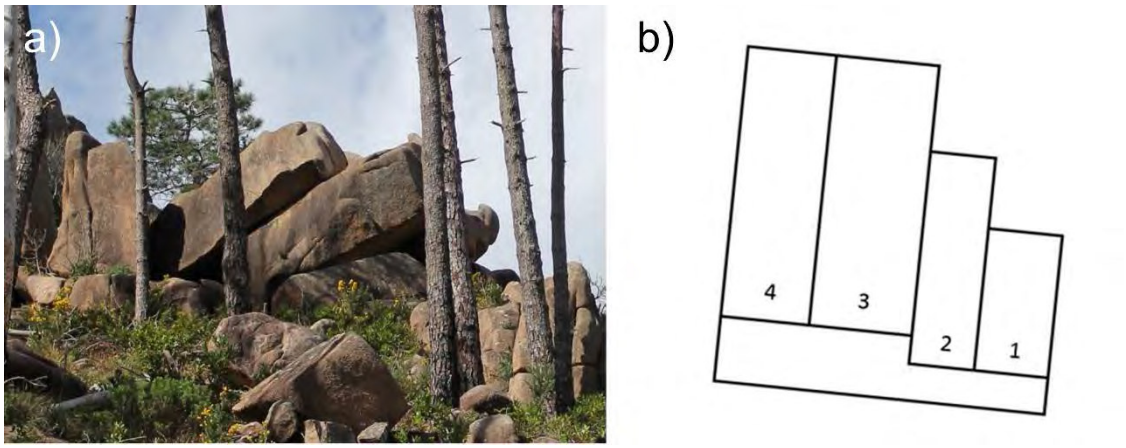

Figure 16. Set of four blocks analysed in case study 1: picture on site (a) and simplified cross-cut view (b).

To analyse the role of the rounded edges in the failure of the set, Goodman and Bray (1976) calculations were performed to obtain the FoS for both rounded and sharp edges. Set geometry (summarized in Table 8) was measured in the field using measuring tape for block dimensions, a set-square for corner rounding, a compass with inclinometer to orientate rock contacts and standard rock mechanics field equipment. Note that the geometry measurements were simplified to make calculations more straightforward, so the results must be taken as an overall estimate.

Table 9. Case study 1 block measurements.

Block	Yn (m)	Δx (m)	r_c (m)
4	3.8	1.2	0.2
3	3.8	1.4	0.3
2	3	0.9	0.23
1	2	1	0.2

Note: Blocks are enumerated from the bottom position to the top position.

Other relevant geometrical parameters were base inclination $\alpha=12^0$, assumed friction angles of the contacts $\phi_b=35^0$ and $\phi_j=30^0$, and rock specific weight $\gamma=25.5$ kN/m^3. The height of the step separating the base of the block 1 and 2 from that of blocks 3 and 4was 40 cm. By using these parameters for the calculations, the FoS values for blocks with sharp edges and rounded edges were found to be 2.71 and 0.93, respectively, thereby justifying the present state of the slope.

5.2. Case study 2

Downhill from the location of the first analysed set of blocks was another set of toppled blocks, stable because a block at the end was preventing further toppling (Figure 17).

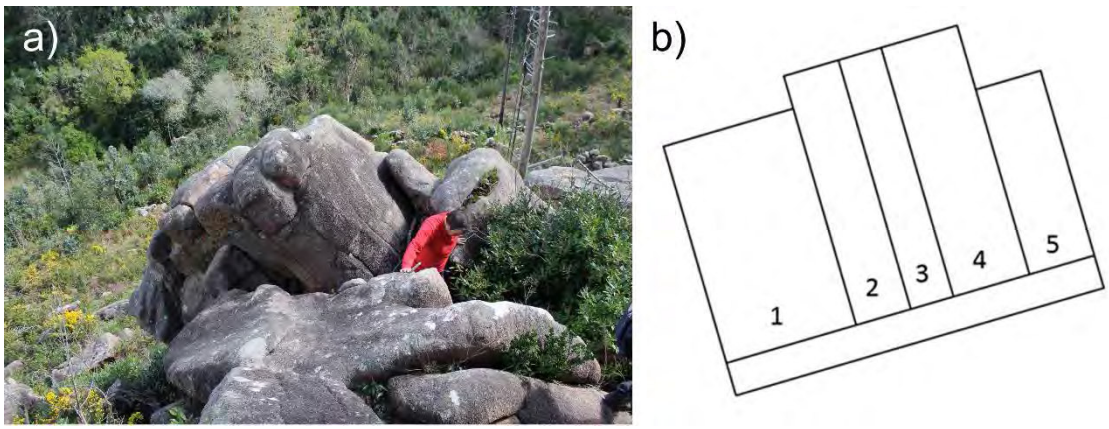

Figure 17. Set of five blocks analysed in case study 2: picture on site (a) and simplified cross-cut view (b).

This second set of five blocks with different thicknesses and sizes was measured for the same parameters as the first set of blocks (Table 9). Specific weight and friction angles were assumed to be the same since they would be typical values for granitic rocks in this location. The base inclination was $\alpha=10^0$ and the base where all the blocks rested was assumed to be planar. The FoS values for blocks with sharp edges and rounded edges were found to be 3.27 and 0.91, respectively, again justifying the present state of the slope and a clear indicator of how rounded corners affected the stability of this natural slope.

Table 10. Case study 2 block measurements.

Block	Yn (m)	Δx (m)	r_c (m)
5	1.7	0.6	0.25
4	2.3	0.7	0.25
3	2.3	0.4	0.2
2	2.3	0.5	0.25
1	2	1.2	0.25

Note: Blocks are enumerated from the bottom position to the top position.

5.3. Discussion of the case study results

The numeric analysis of the two block sets observed in the field revealed a considerable reduction in the FoS after weathering when compared to the FoS before weathering. In the first case, the FoS dropped from 2.71, indicating stability, to 0.93, indicating instability. Similar results were obtained for the second case, in which the initial FoS of 3.27 fell to 0.91 when edge rounding was taken into account.

From these results, it can be concluded that weathering resulting in rounded edges was decisive in the failure of these sets of blocks. Water from rainfall — very frequent in this area — may also have had some influence on the failure mechanisms.

6. Conclusions

Although the role played by rounded edges in the stability of rock slopes prone to block toppling has featured in the literature, as far as we are aware, no comprehensive approach to rigorously analysing this type of problem has been reported. In this study, stability against toppling by blocks with rounded edges was assessed from the analytical and modelling perspectives at laboratory scale and briefly at field scale.

On the analytical side, the Goodman and Bray (1976) limit equilibrium equations for stability against block toppling were revisited, with a modification introduced to take into account the rounding of block edges.

For physical models tilt-tested in the laboratory, it was observed that the rounded-edge model was significantly less stable than the sharp-edge model. When equation accuracy was checked against the analytical approach, we found a standard deviation of 1^0, which is quite an acceptable value for the rock mechanics discipline.

It could also be observed that the impact of edge rounding on stability largely depended on the overall slope geometry and on the friction angles, particularly for the contact base. When sliding was more relevant, the influence of rounded edges was limited. As demonstrated in two case studies of granite blocks on a natural slope, for a small number of not-so-slender blocks, the impact of rounded edges on stability tends to grow dramatically. Likewise, rounded corners do not play a significant role when there is a large number of slender blocks but they do for a small number of thicker blocks.

In view of our analysis, it can be concluded that — using the expressions presented in this article — the role played by the rounding of block corners can be incorporated with a reasonable level of accuracy in both analytical approaches to single block stability and stability analyses of toppling.

Acknowledgements

The authors Leandro. R. Alejano Monge and Ignacio Pérez Rey thank the Spanish Ministry of the Economy, Industry and Competitiveness for partial funding of this study (Contract Reference No. BIA2014-53368-P), in turn partially financed by ERDF funds. Thanks to Carlos Carranza–Torres from University of Minnesota-Duluth (USA) for providing a

calculation sheet implementing a version of the Goodman and Bray's method considering rounded corners. Ailish M. J. Maher is acknowledged for English language editing of a version of this manuscript.

7. References

Alejano, L.R, Alonso, E., 2005. Application of the 'shear and tensile strength reduction technique' to obtain factors of safety of toppling and footwall rock slopes, in: Konecny, P. (Ed.), Impact of Human Activity on the Geological Environment EUROCK 2005: Proceedings of the International Symposium EUROCK 2005, Taylor and Francis Group, London, pp. 7-13.

Alejano, L.R., Carranza-Torres, C., Giani, G.P., Arzúa, J., 2015. Study of the stability against toppling of rock blocks with rounded edges based on analytical and experimental approaches. Eng Geol. 195 (2015), 172–184.

Alejano, L.R., Ferrero, A.M., Ramírez-Oyanguren, P., Álvarez Fernández, M.I., 2011. Comparison of limit-equilibrium, numerical and physical models of wall slope stability. Int. J. Rock Mech. Min. 48, 16-26.

Alejano, L.R., Gómez-Márquez, I., Martínez-Alegría, R., 2010. Analysis of a complex toppling-circular slope failure. Eng. Geol. 114, 93–104.

Alejano, L.R., González, J., Muralha, J., 2012. Comparison of Different Techniques of Tilt Testing and Basic Friction Angle Variability Assessment. Rock Mech. Rock Eng. 45, 1023–1035.

Ashby, J., 1971. Sliding and Toppling Modes of Failure in Model and Jointed Rock Slopes. (MSc Thesis). Imperial College London, London.

Böhme, M., Hermanns, R.L., Oppikofer, T., Fischer, L., Bunkholt, H.S.S., Eiken, T., Pedrazzini, A., Derron, M.H., Jaboyedoff, M., Blikra, L.H., Nilsen, B., 2013. Analyzing complex rock slope deformation at Stampa, western Norway, by integrating geomorphology, kinematics and numerical modelling. Eng Geol. 154, 116–130.

Coulthard, M.A., Dugan, K.J. and Hutchison, B.J., 2001. Numerical modelling of complex slope movements at Savage River Mine, Tasmania, in: Contractor, D., Desai, C.S., Harpalani, S., Kemeny, J., Kundu, T. (Eds.), Proceedings of the 10th International Conference on Computer Methods and Advances in Geomechanics, Tucson, U.S.A., pp. 1673–1678.

Cravero, M., Iabichino, G., Nacci, F., Rinaldi, L., Vigliero, L., 2003. Analysis of a rock slope failure in a feldspar open-pit mine ISRM 2003–Technology roadmap for rock mechanics, South African Institute of Mining and Metallurgy, 2003.

Cruden, D.M., Hu, X.Q., 1994. Topples on underdip slope in the Highwood Pass, Alberta, Canada. Q. J. Eng. Geol. 27:57–68.

De Freitas, M.H., Waters, J., 1973. Some field examples of toppling failure. Géotechnique, 23: 495–514.

Giraud, A., Rochet, L., Antoine. P., 1990. Processes of slope failure in crystallophyllian formations. Eng. Geol. 29, 241–253.

Gischig, V., Amann, F., Moore, J.R., Loew, S., Eisenbeiss, H., Stempfhuber, W., 2011. Composite rock slope kinematics at the current Randa instability, Switzerland, based on remote sensing and numerical modeling. Eng. Geol. 118 (1-2), 37–53.

Goodman, R.E., Bray, J.W., 1976. Toppling of Rock Slopes in Rock Engineering for Foundation and Slopes, Special Conference ASCE, Boulder Colorado, Vol. 2, pp. 201–234.

Gu, D., Huang, D., 2016. A complex rock topple-rock slide failure of an anaclinal rock slope in the Wu Gorge, Yangtze River, China. Eng. Geol. 208, 165–180.

Hencher, S.R., 2012. Discussion of Alejano, Gonzalez and Muralha (2012). Rock Mech. Rock Eng. (2012). 45, 1137–1139.

Hencher, S.R, 2012b. Practical Engineering Geology. Balkema, Rotterdam.

Hoek, E., Bray, J., 1974. Rock Slope Engineering. Institution of Mining and Metallurgy, London.

Hutchison, B., Dugan, K., Coulthard, M.A., 2000. Analysis of flexural toppling at Australian bulk minerals Savage River Mine, GeoEng2000, Int. Conf. Geotech. Geol. Eng. CDROM Paper 6, Melbourne.

Itasca, 2010. User manual for UDEC, Version 5.0. Itasca Cons. Group Inc., Minnesota.

Jones, T. R., 1859. Notes on some granite rock masses. J. Geol. 45, 625–635.

León-Buendía, C., Santamaría-Arias, J., Alejano, L.R., Giráldez, R., 2014. Analysis of a complex slope failure in a quartzite slope, in: Alejano, L.R., Perucho, A., Olalla, C., Jiménez, R.,(Eds.), Rock Engineering and Rock Mechanics: Structures in and on Rock Masses: Proceedings of EUROCK 2014. pp. 1207–1211.

Manera Bassa, C., Oyanguren, P.R., Philippon, R.G., Fernández-Pello, Lois M., 2014. The toppling of large blocks on the northeast slope of the Meirama mine. in: Alejano, L.R., Perucho, A., Olalla, C., Jiménez, R.,(Eds.), Rock Engineering and Rock Mechanics: Structures in and on Rock Masses: Proceedings of EUROCK 2014., pp. 731–736.

Martin, D.C., 1990. Deformation of open pit mine slopes by deep-seated toppling. Int. J. of Surf. Min. & Reclam. 4, 153–164.

Mohtarami, E., Jafari, A., Amini, M., 2014. Stability analysis of slopes against combined circular-toppling failure. Int. J. Rock Mech. Min. 67, 43–56.

Ollier, C.D., 1975. Weathering. Longman, London.

Pueyo–Morer, E., Román-Berdiel, T., Casas-Sainz, A.M., 1995. Granite intrusion contemporary to shortening and normal extension in the Iberian Hercynian Massif. European Union of Geosciences 8th meeting. Abstracts supplement No 1 to Terra Nova. Pp. 143.

Sagaseta, C., Sánchez, J.M., Cañizal, J., 2001. A general analytical solution for the required anchor force in rock slopes with toppling failure. Int. J. Rock. Mech. Min. 38 (3), 421–435.

Sanz de Galdeano, C., 1990. Geologic evolution of the Betic Cordilleras in the Western Mediterranean, Miocene to the present. Tectonophysics. 172, 107–119. https://doi.org/10.1016/0040-1951 (90)90062-D.

Selby, M.J., 1993. Hillslope Materials and Processes, Oxford University Press, Oxford.

Sjöberg, J., 1999. Analysis of large-scale rock slopes. (PhD thesis). Technical University of Lulea, Sweden.

Stead, D., Eberhardt, E., Coggan, J.S., 2006. Developments in the characterization of complex rock slope deformation and failure using numerical modelling techniques. Eng. Geol. 83 (2006), 217–235.

Twidale, C.R. and Vidal Romaní, J.R., 2005. Landforms and Geology of Granite Terrains. Balkema, Rotterdam.

Vidal Romaní, J.R., 1989. Granite geomorphology in Galicia NW Spain. Cadernos do Laboratorio Xeolóxico de Laxe. 13, 89–163.

Vidal Romaní, J.R., Brum Ferreira, A., Zezere, J.L., Rodrígues, L. & Monge, C., 1990. Evolución cuaternaria del relieve granítico en la Serra de Gerês-Xurés (Minho, Portugal-Ourense, Galicia). [Quaternary evolution of granitic topography in Serra de Gerês-Xurés (Minho, Portugal-Ourense, Galicia)]. Cuaternario y Geomorfología. 4, 3–12.

Wyllie, D.C., Mah, C.W., 2004. Rock Slope Engineering (Civil and Mining), fourth ed. Taylor and Francis Group, London.

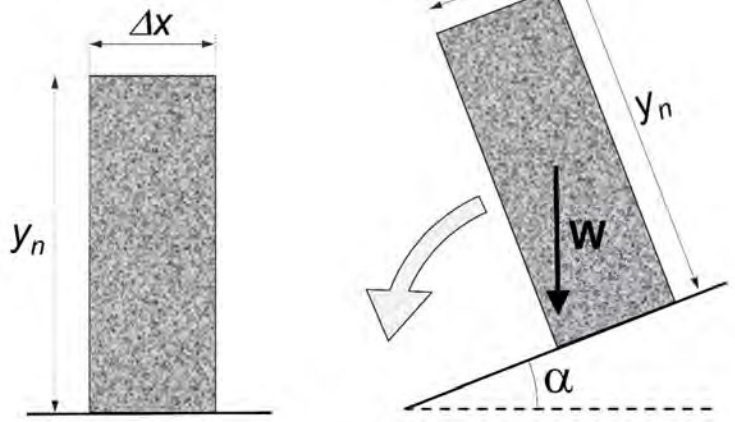

$$FoS = \frac{M_{stab}}{M_{overt}} = \frac{W \cos\alpha \dfrac{\Delta x}{2}}{W \sin\alpha \dfrac{Y_n}{2}} = \tan^{-1}\alpha \frac{\Delta x}{Y_n} \quad (1)$$

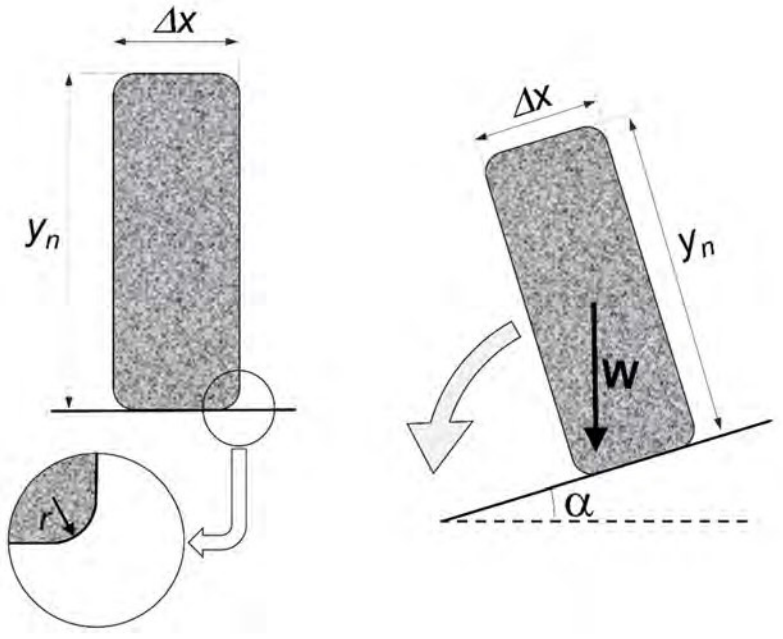

$$FoS = \frac{M_{stab}}{M_{overt}} = \frac{W \cos\alpha \left(\dfrac{\Delta x}{2} - r\right)}{W \sin\alpha \dfrac{Y_n}{2}} = \tan^{-1}\alpha \frac{\Delta x - 2r}{Y_n} \quad (2)$$

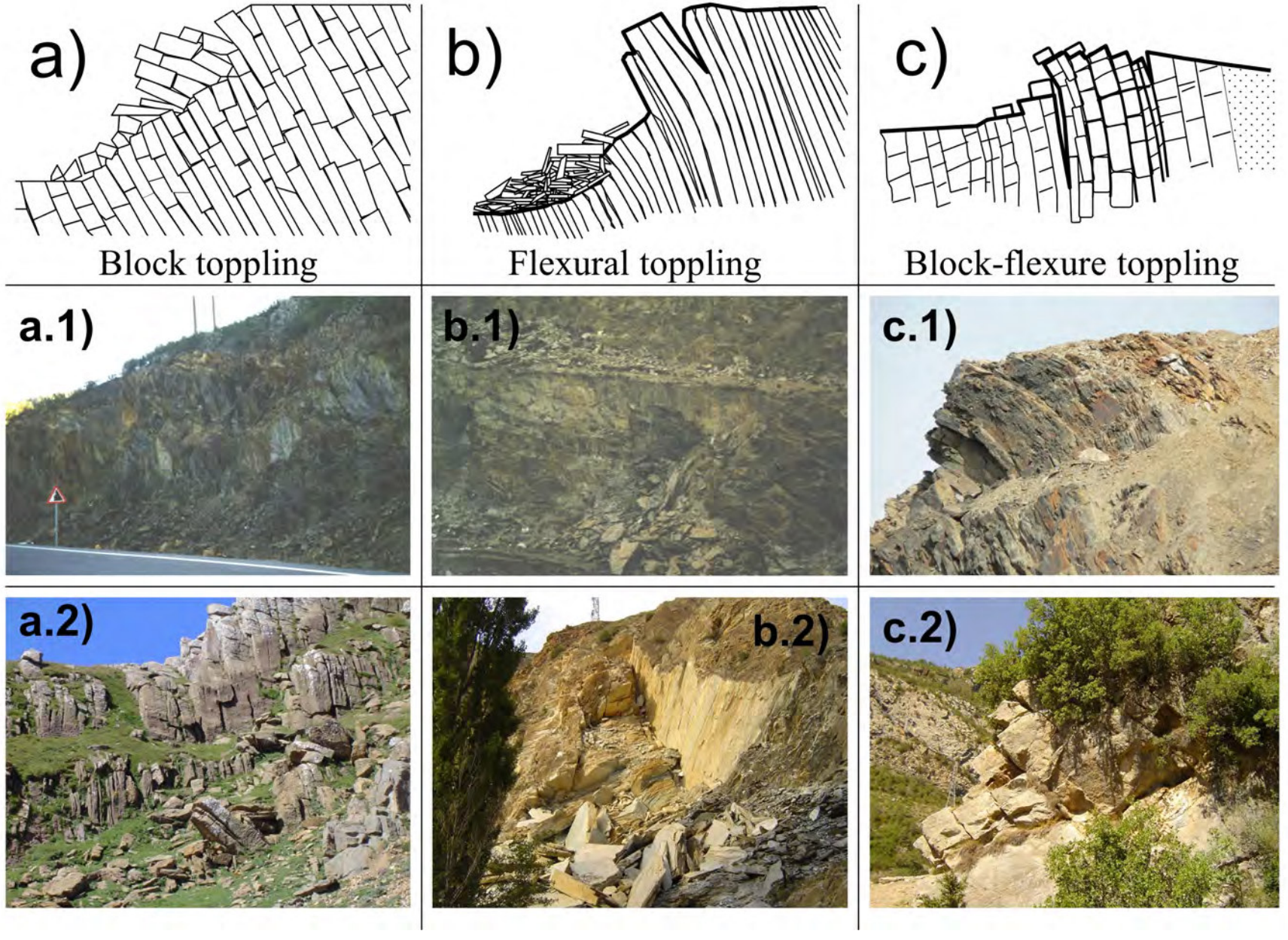
a)
b)
c)
Block toppling
Flexural toppling
Block-flexure toppling
a.1)
b.1)
c.1)
a.2)
b.2)
c.2)

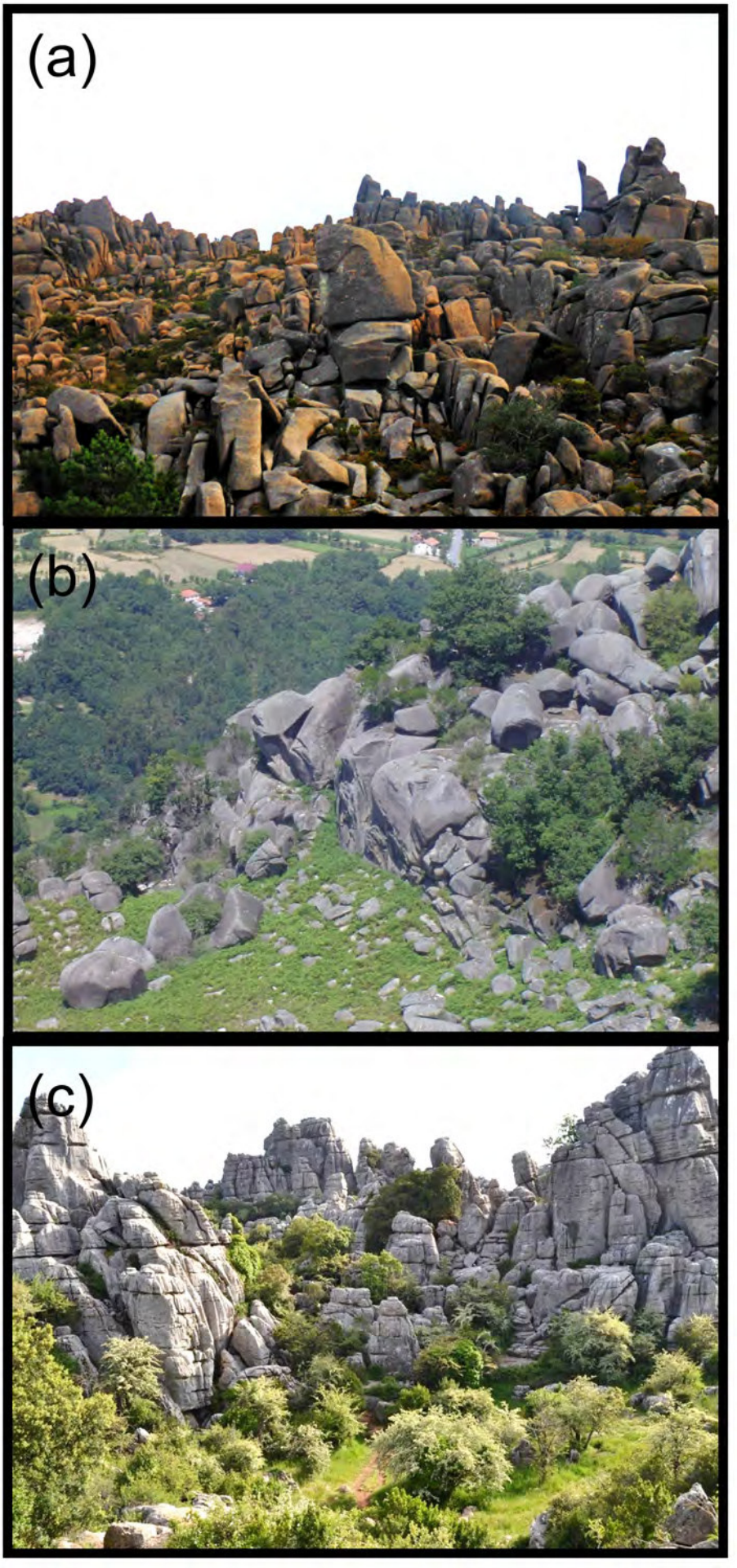
(a)
(b)
(c)

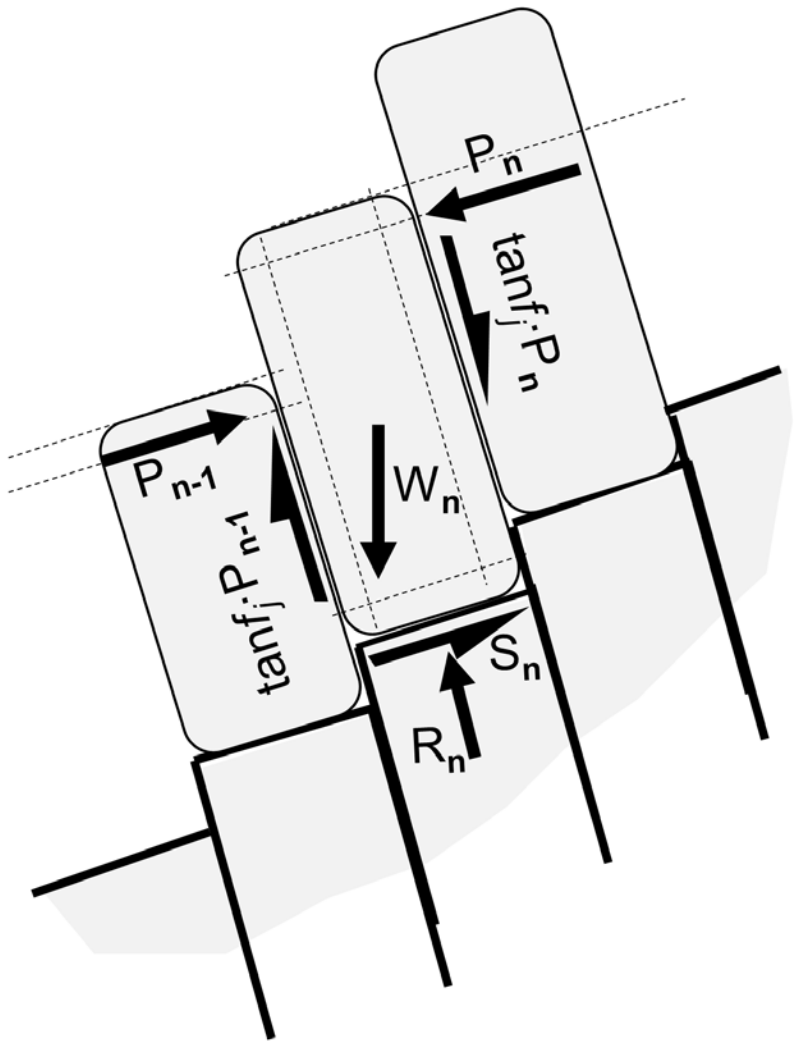
P_n
$tanf_j \cdot P_n$
P_{n-1}
$tanf_j \cdot P_{n-1}$
W_n
S_n
R_n

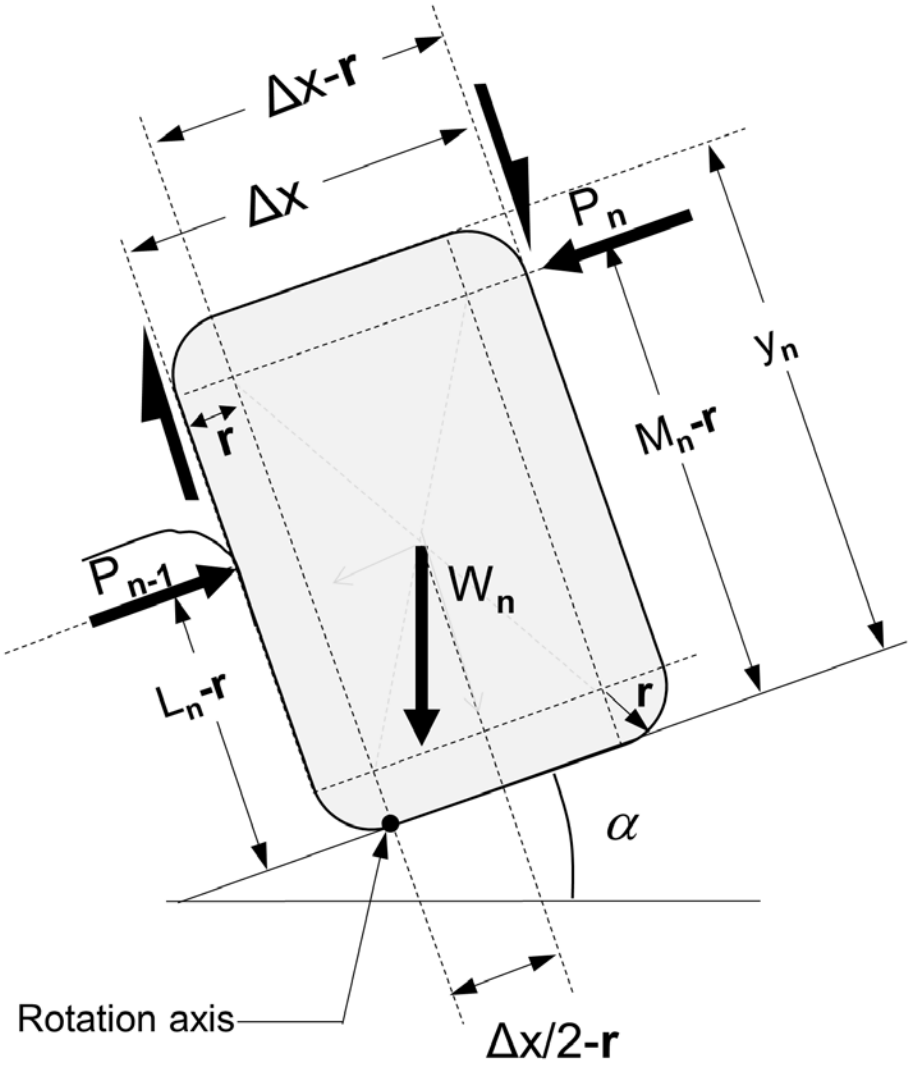
Δx-**r**
Δx
P_n
y_n
M_n-**r**
r
P_{n-1}
W_n
L_n-**r**
r
α
Rotation axis
$\Delta x/2$-**r**

a)

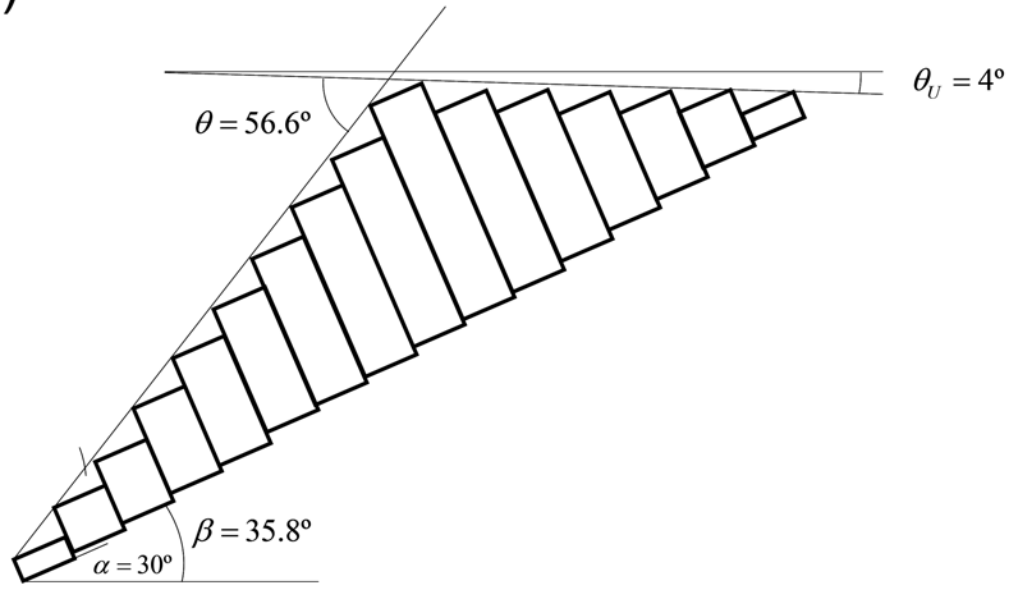
$\theta_U = 4^o$
$\theta = 56.6^o$
$\beta = 35.8^o$
$\alpha = 30^o$

b)

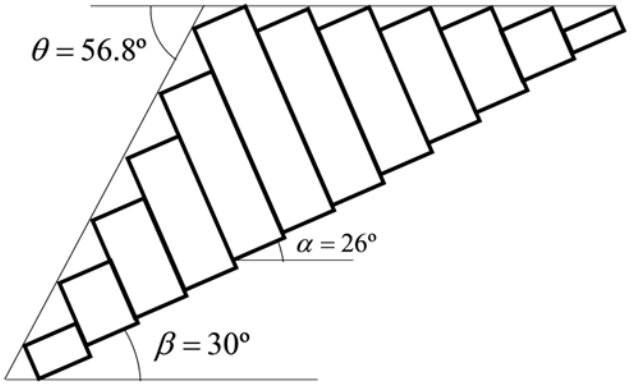
$\theta = 56.8^o$
$\alpha = 26^o$
$\beta = 30^o$

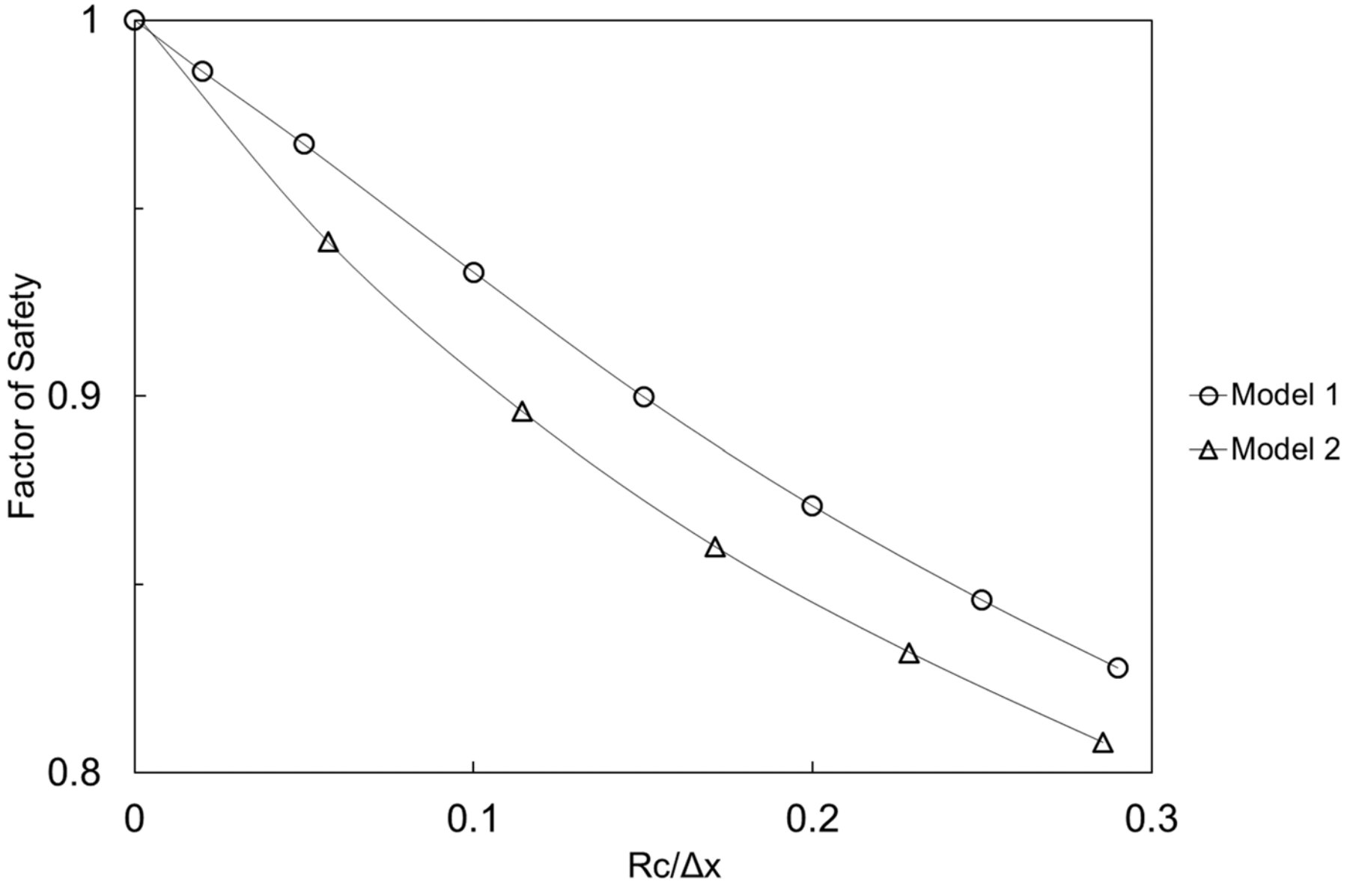
1
0.9
0.8
Factor of Safety
0
0.1
0.2
0.3
Rc/Δx
Model 1
Model 2


(a)
1
2
3
4
5
6
7
8
9
10
(b)
1
2
3
4
5
6
7
8
9
10

MODEL – PLANAR BASE

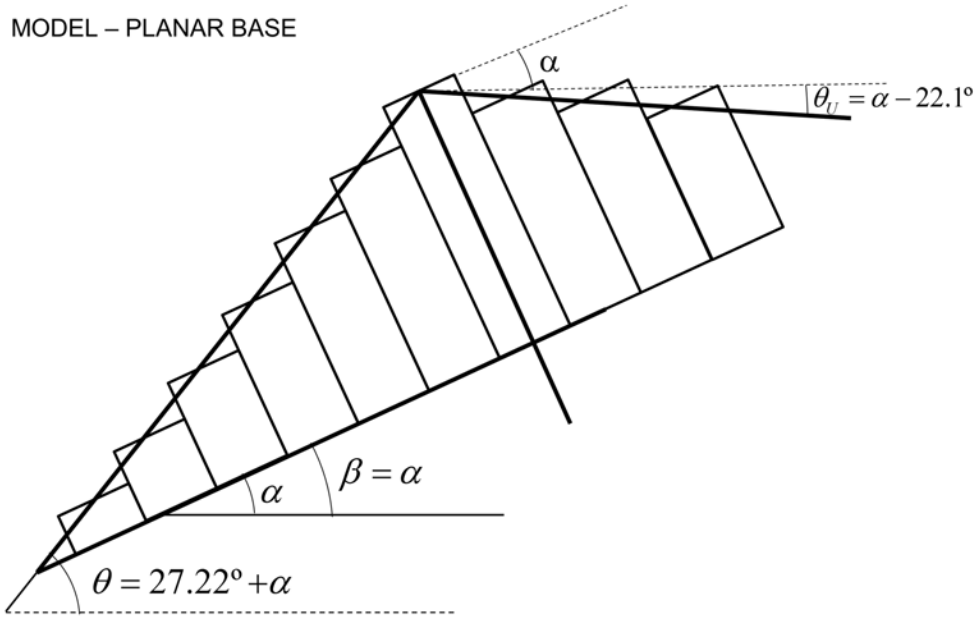

MODEL – STEPPED BASE

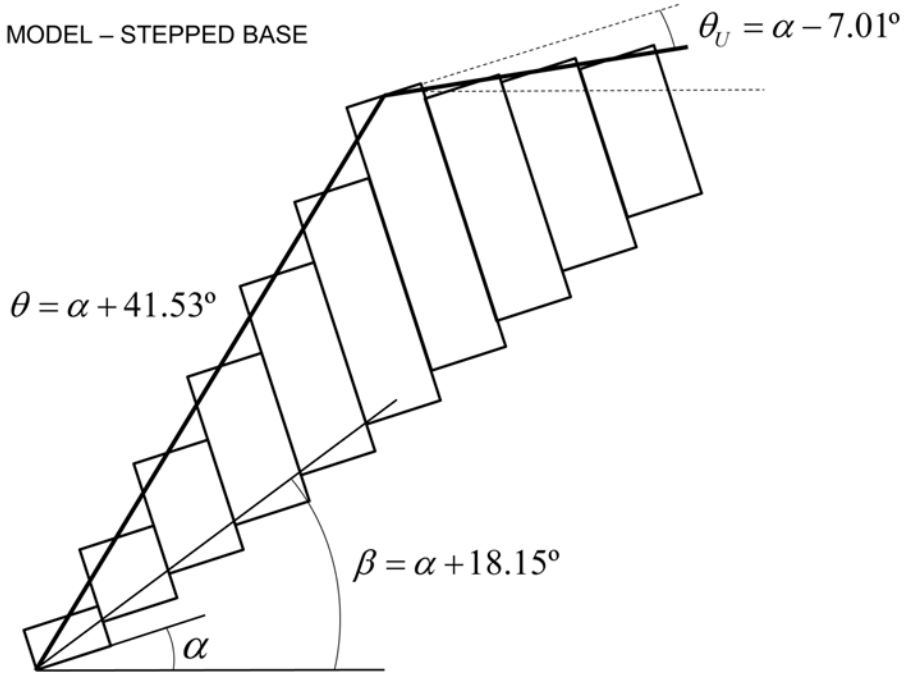

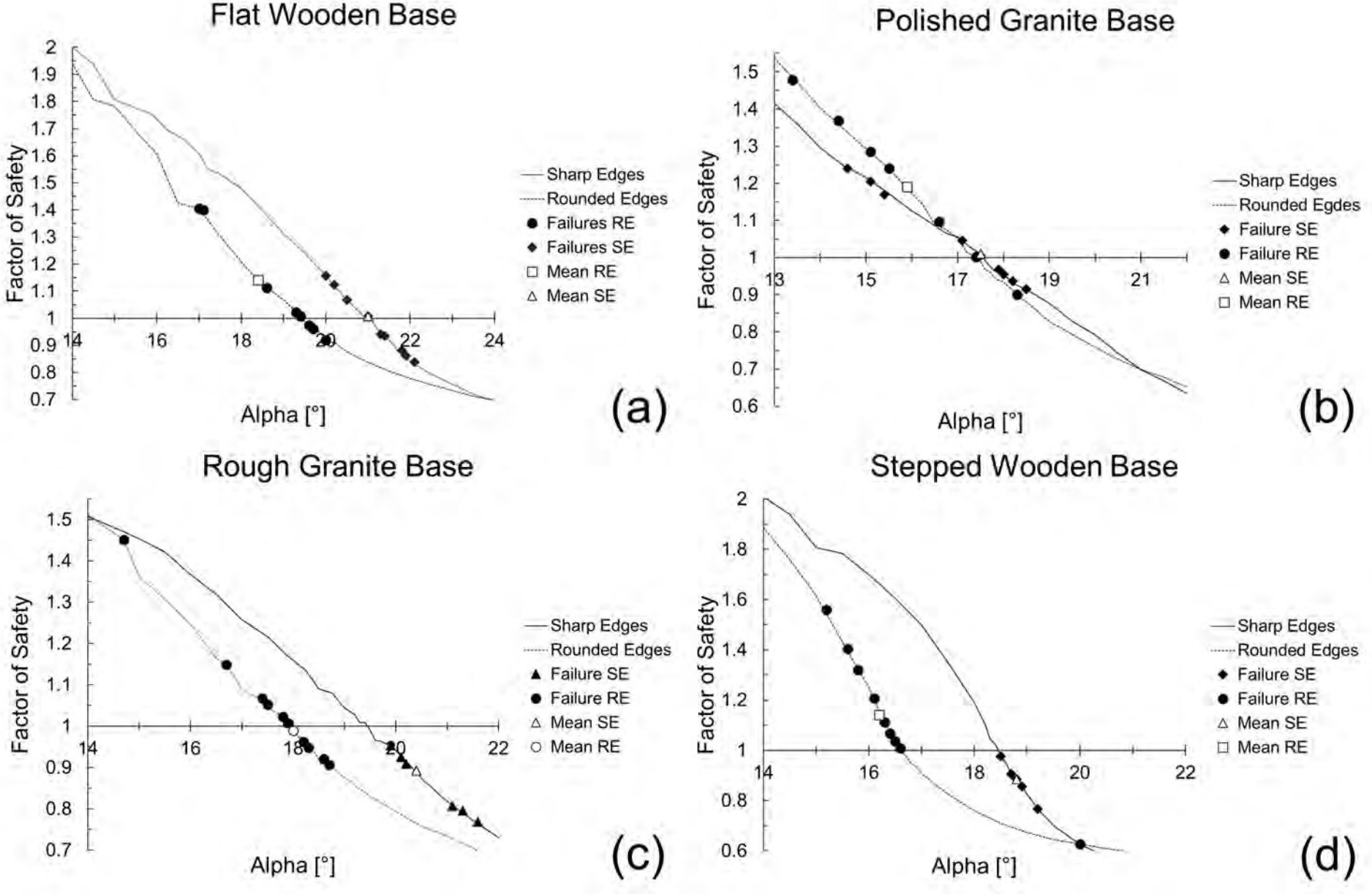
Flat Wooden Base
Factor of Safety
Alpha [°]
Sharp Edges
Rounded Edges
Failures RE
Failures SE
Mean RE
Mean SE
(a)
Polished Granite Base
Factor of Safety
Alpha [°]
Sharp Edges
Rounded Egdes
Failure SE
Failure RE
Mean SE
Mean RE
(b)
Rough Granite Base
Factor of Safety
Alpha [°]
Sharp Edges
Rounded Edges
Failure SE
Failure RE
Mean SE
Mean RE
(c)
Stepped Wooden Base
Factor of Safety
Alpha [°]
Sharp Edges
Rounded Edges
Failure SE
Failure RE
Mean SE
Mean RE
(d)

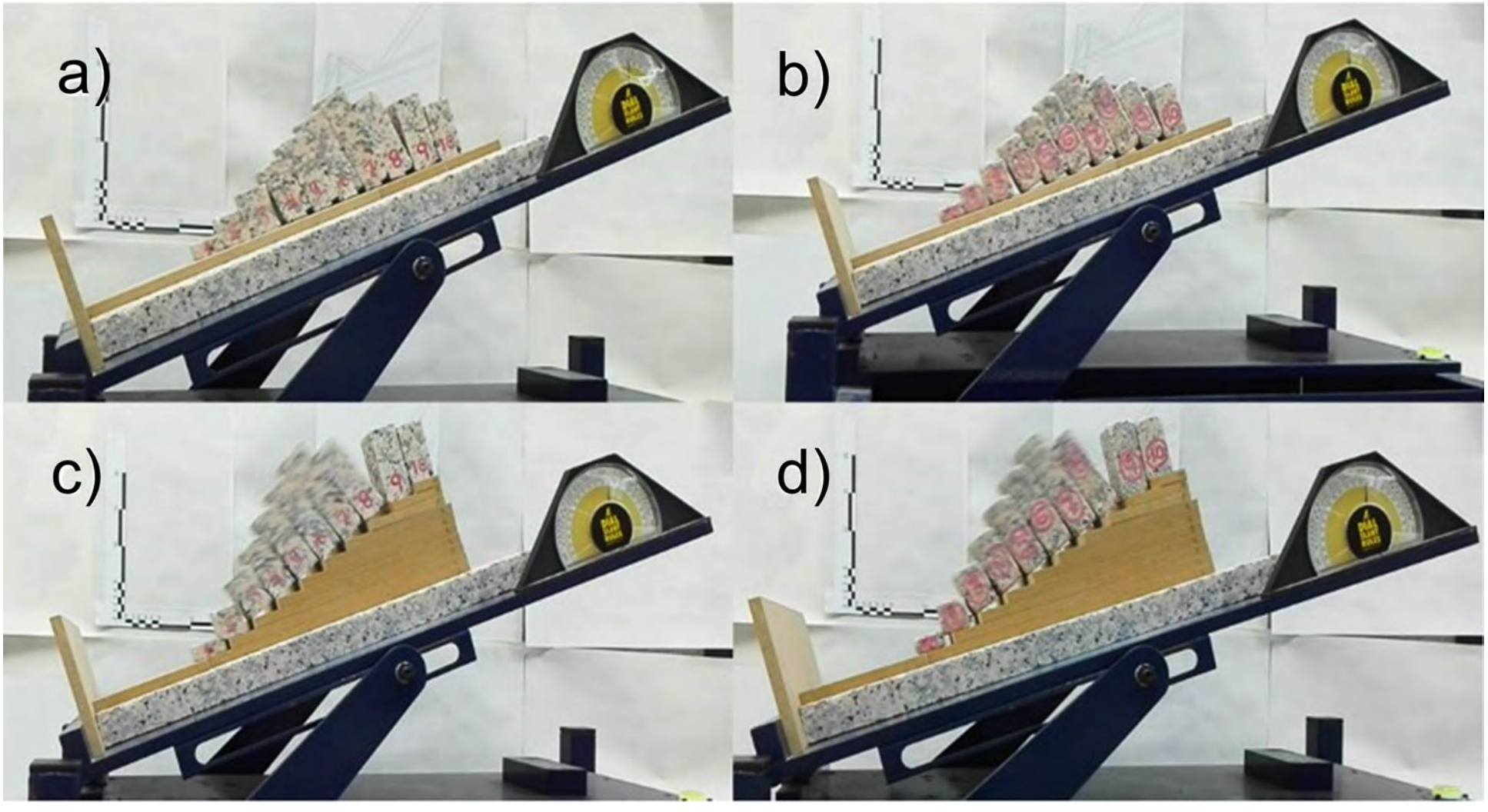
a)
b)
c)
d)


a)

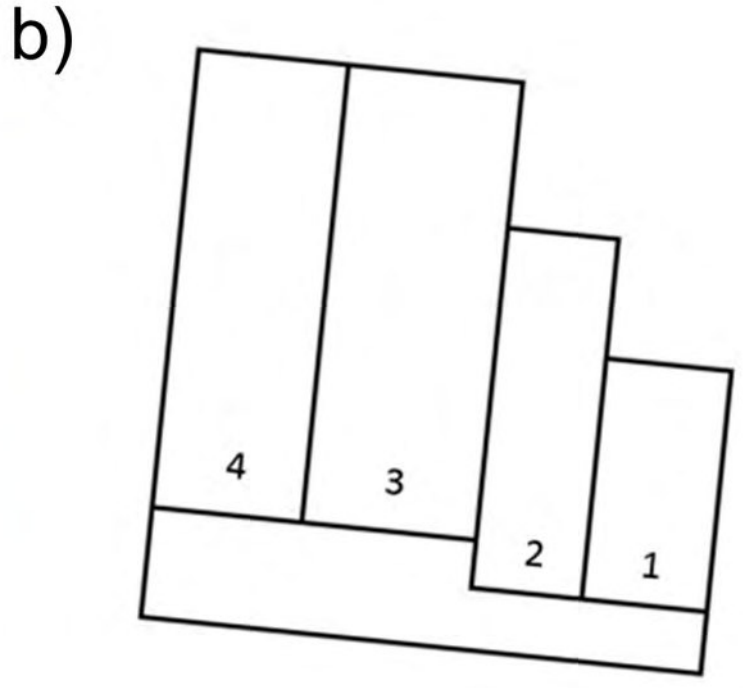
b)
4
3
2
1


a)

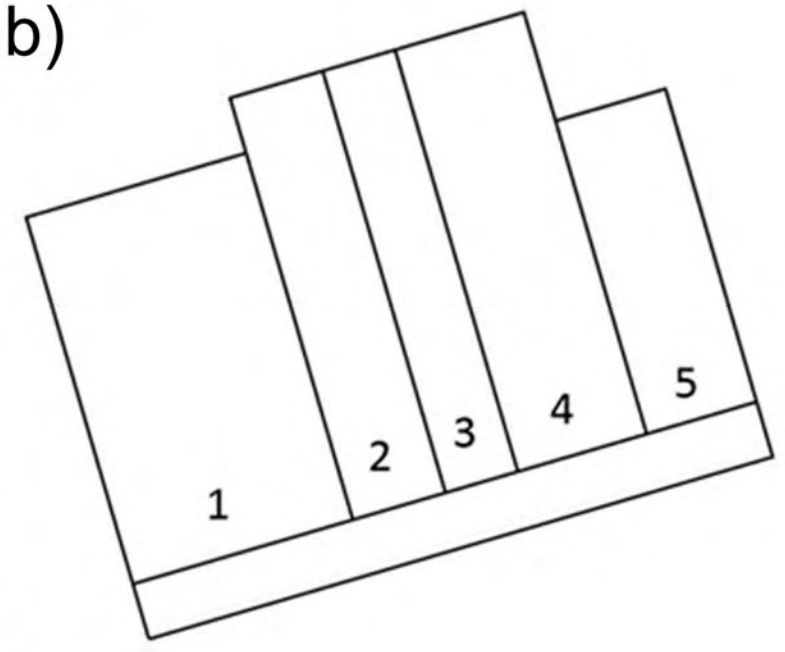
b)
1
2
3
4
5

Table 1. Geometrical and weight data for the sharp-edge blocks.

Block #	B	L	H	Weight	Submerged weight	Density from sunken weight
	[mm]	[mm]	[mm]	[g]	[g]	[g/cm^3]
1	31.21	47.74	15.66	60.13	37.36	2.64
2	31.06	47.77	30.36	116.64	72.2	2.62
3	31.10	47.56	47.50	169.73	104.85	2.62
4	31.17	47.89	59.34	229.4	141.86	2.62
5	31.23	47.64	75.36	290.37	179.61	2.62
6	31.37	47.92	89.84	349.8	216.4	2.62
7	31.35	47.90	104.31	404.7	250.18	2.62
8	31.33	48.14	89.50	349.04	215.76	2.62
9	31.20	47.65	74.42	285.97	178.83	2.67
10	31.13	47.65	59.97	230.16	142.44	2.62
					Average	2.63

Table 2. Geometrical and weight data for rounded-edge blocks.

Block #	B	L	H	Weight	Submerged weight	Density from sunken weight
	[mm]	[mm]	[mm]	[g]	[g]	[g/cm^3]
1	31.27	47.80	15.74	58.3	36.52	2.67
2	31.09	47.78	30.41	112.8	70.08	2.64
3	31.10	47.55	44.63	164.1	100.71	2.59
4	31.17	48.32	59.42	225.2	137.85	2.58
5	31.35	47.77	64.83	288.2	175.97	2.57
6	31.34	48.26	89.72	345.3	212.93	2.61
7	31.40	47.50	104.27	404.6	247.56	2.58
8	31.38	47.97	89.48	345.3	210.64	2.56
9	31.22	47.52	74.50	284.0	174.4	2.59
10	31.20	47.71	60.06	229.8	142.16	2.62
					Average	2.60

Table 3. Original and final weights of blocks after slaking and radius of curvature calculation results.

Block #	Weight of sharp-edge block	Weight of rounded-edge block	Weight loss	Average radius of circular rounding	Operative radius of curvature
	[g]	[g]	[%]	[mm]	[mm]
1	60.13	58.33	2.99	2.916	1.944
2	116.63	112.76	3.32	3.955	2.637
3	169.71	164.11	3.30	4.490	2.990
4	229.38	225.24	1.80	3.653	2.435
5	290.35	288.16	0.75	2.423	1.62
6	349.79	345.34	1.27	3.425	2.28
7	410.81	404.62	1.51	3.841	2.56
8	349.01	345.27	1.07	3.140	2.09
9	285.97	284.01	0.68	2.389	1.593
10	230.14	229.78	0.16	1.080	0.72
		Average	1.70	3.13	2.09
		Std. Dev.	1.14	0.983	

Table 4. Friction angle estimates for contacts with different bases and for joints.

Test #	Sharp Edges				Rounded Edges			
	Wooden Base	Rough Granite	Polished Granite	Block Joints	Wooden base	Rough Granite	Polished Granite	Block Joints
1	26.8	23.9	18.5	18.2	26.8	20.3	23.5	24.9
2	32.3	22.1	22.0	17.8	26.7	18.5	19.3	27.5
3	26.4	20.9	16.0	19.9	23.6	21.6	19.7	27
4	25.9	17.9	17.6	21.6	25.1	21.2	17.5	26.2
Median	26.6	21.5	18.05	19.05	25.9	20.75	19.5	26.6
Average	27.85	21.2	18.52	19.37	25.55	20.4	20	26.4
St. Dev.	2.99	2.52	2.54	1.74	1.52	1.38	2.52	1.13

Table 5. Sharp-edge model results for four different bases.

Base	Flat Wooden		Rough Granite		Polished Granite		Stepped Wooden	
Position	Normal	Upside Down	Normal	Upside Down	Normal	Upside Down	Normal	Upside Down
1	21.8	21.9	20.4	21.1	18.2	17.9	19.2	18.9
2	21.4	20	21.6	21.3	18	18.5	18.7	18.8
3	21.3	20.5	20.1	19.9	14.6	15.4	19.2	18.5
4	21.9	22.1	20.4	20.2	17.5	17.1	18.7	18.5
5	21	20.2	19.9	20.4	15.1	17.5	18.8	18.8
Median	21.4	20.5	20.4	20.4	17.5	17.5	18.8	18.8
Average	21.48	20.94	20.48	20.58	16.68	17.28	18.92	18.7
St Dev	0.370	0.986	0.661	0.597	1.699	1.171	0.259	0.187

Table 6. Rounded-edge model results for four different bases.

Base	Flat Wooden		Rough Granite		Polished Granite		Stepped Wooden	
Position	Normal	Upside Down	Normal	Upside Down	Normal	Upside Down	Normal	Upside Down
1	19.40	17.10	17.80	18.30	15.50	16.60	16.40	15.80
2	19.70	19.30	14.70	16.70	13.40	17.40	20.00	15.20
3	19.60	17.10	18.60	17.40	14.40	17.40	16.30	16.50
4	20.00	17.00	17.50	18.20	15.10	17.40	16.60	15.60
5	18.60	20.00	17.90	18.70	12.20	18.30	16.60	16.10
Median	19.6	17.1	17.8	18.2	14.4	17.4	16.6	15.8
Average	19.46	18.1	17.3	17.86	14.12	17.42	17.18	15.84
St Dev	0.527	1.437	1.508	0.802	1.337	0.602	1.582	0.493

Table 7. Average values of results shown in Tables 5 and 6.

Base	Sharp-Edge Model			Rounded-Edge Model		
	Prediction	Results		Prediction	Results	
Flat Wooden	20.9	21.4	20.5	19.4	19.6	17.1
Rough Granite	19.4	20.4	20.4	17.9	17.8	18.2
Polished Granite	17.5	17.5	17.5	17.4	14.4	17.4
Stepped Wooden	18.7	18.8	18.8	16.6	16.6	15.8

Table 8. Summarized failure mechanisms for the models reflected in Figure 13. T stands for theoretical and L for laboratory.

Block	**Sharp-Edge Models**				**Rounded-Edge Models**			
	Flat Wooden Base		Stepped Wooden Base		Flat Wooden Base		Stepped Wooden Base	
	T	**L**	**T**	**L**	**T**	**L**	**T**	**L**
10	Stable	Stable	Stable	Stable	Stable	Stable	Stable	Stable
9	Toppling	Toppling	Stable	Stable	Toppling	Toppling	Toppling	Stable
8	Toppling	Toppling	Toppling	Toppling	Toppling	Toppling	Toppling	Toppling
7	Toppling	Toppling	Toppling	Toppling	Toppling	Toppling	Toppling	Toppling
6	Toppling	Toppling	Toppling	Toppling	Toppling	Toppling	Toppling	Toppling
5	Toppling	Toppling	Toppling	Toppling	Toppling	Toppling	Toppling	Toppling
4	Toppling	Toppling	Toppling	Toppling	Toppling	Toppling	Toppling	Toppling
3	Sliding	Sliding	Toppling	Toppling	Toppling	Sliding	Toppling	Toppling
2	Sliding	Sliding	Sliding	Sliding	Sliding	Sliding	Sliding	Sliding
1	Sliding	Sliding	Sliding	Sliding	Sliding	Sliding	Sliding	Sliding

Table 9. Case study 1 block measurements.

Block	Yn (m)	Δx (m)	r_c (m)
4	3.8	1.2	0.2
3	3.8	1.4	0.3
2	3	0.9	0.23
1	2	1	0.2

Note: Blocks are enumerated from the bottom position to the top position.

Table 10. Case study 2 block measurements.

Block	Yn (m)	Δx (m)	r_c (m)
5	1.7	0.6	0.25
4	2.3	0.7	0.25
3	2.3	0.4	0.2
2	2.3	0.5	0.25
1	2	1.2	0.25

Note: Blocks are enumerated from the bottom position to the top position.